Activation of 96-Well Polypropylene Plates with Radio Frequency Plasma Ion Etching to Increase Chromatin Binding Capacity for Immunoprecipitation

Theodore Schrimshire

A thesis

submitted in partial fulfillment of the

requirements for the degree of

Master of Science in Bioengineering

University of Washington

2023

Committee:

Dr. Karol Bomsztyk

Dr. Oleg Denisenko

Dr. Lara Gamble

Program Authorized to Offer Degree:

Bioengineering

University of Washington

Abstract

Activation of 96-Well Polypropylene Plates with Radio Frequency Plasma Ion Etching to Increase Chromatin Binding Capacity for Immunoprecipitation

Theodore Schrimshire
Chair of the Supervisory Committee:
Karol Bomsztyk
Departments of Medicine, Pharmacology, and Bioengineering

Background Chromatin Immunoprecipitation (ChIP) is an assay that can quantify epigenetic alterations. The Bomsztyk lab has developed technology for high-throughput chromatin immunoprecipitation (ChIP) microplate-based assays called PIXUL-Matrix-ChIP. These assays use 96-well polypropylene (PP) sample plates that are treated with 48 hours of UV light irradiation to activate the surface for the absorption of antibodies that immunoprecipitate chromatin. Plasma reactive ion etching (RIE) is a potential alternative treatment method that can activate PP by adding highly polar oxygen species to the surface in a small fraction of the time compared to UV treatment.
Methods This report investigates the use of oxide-plasma treatments to activate the surface of the PP plates to reduce plate treatment times to less than 5 minutes and ideally increase the ChIP assay efficiency. I used plasma etching to increase the molecular polarity of the surface so more antibodies can bind to the PP and increase the capacity for chromatin immunoprecipitation. To assess surface properties after UV vs plasma treatments, I used water contact angle measurements (WCA), X-ray spectroscopy (XPS), and surface roughness estimation. I used chromatin from serum-treated HCT116 in Matrix ChIP to assess the antibody binding capacity of the PP after treatments based on ChIP signal response and background noise.
Results The UV-treated PP had higher hydrophilicity (WCA) and higher oxygen content and surface polarity (XPS) than tested doses of plasma treatment, PP surface qualities produced by 1 min of plasma treatment which were closest to those yielded by 48 hours of UV. The ChIP data for the UV and 1 min plasma treated plates show the expected immunoprecipitation signal for the well-studied gene sites and antibodies (Pol II: EGR1 exon1-5 and 2-3, H3: all three sites, CTCF: EGR1 -15kb) and a low signal at the unspecific background level which is the assay noise (non-immune IgGs: all sites). Among the examined surface qualities, the hydrophilicity and oxygen content are the major factors in the treated PP surface that correlate with the capacity of antibodies absorption which determines the efficiency of chromatin immunoprecipitation.
Conclusions The 1 min plasma-treated plates outperformed 48 hrs UV treatment by 11-20 percent in ChIP assay (noise adjusted signal). While these data show promise, testing other plasma treatment conditions (duration, oxygen concentration, and others) will be required to replace UV treatment in quality and reliability.

Introduction:

Cancer is a set of diseases that are defined by abnormal cell division that is uncontrollable causing damage to surrounding tissues and death. Common cancers include lung cancer, colon cancer, breast cancer, and prostate cancer. Cancer is the second leading cause of death in the United States and a major public health problem around the world [1]. The major factors that contribute to the likelihood of a person getting cancer include age, genetics, and carcinogen exposure. Ultraviolet light from sun exposure is a common source of physical carcinogens. Atmospheric pollutants, asbestos, tobacco smoke, and arsenic are common chemical carcinogens and can be introduced to the body through consumption whether intentional or accidental. Biological carcinogens can include viruses, parasites, or bacteria that can cause serious infections and increase the likelihood of cancer. As individuals age, there can be a buildup of cancer risks and a decrease in cellular function and cellular repair, which can increase the likelihood of getting cancer [2]. Worldwide, cancer is also the second leading cause of death. 2021 Data from the World Health Organization shows that the most common cancers are breast cancer with 2.26 million cases, lung cancer with 2.21 million cases, colon, and rectum cancer with 1.93 million cases, prostate cancer with 1.41 million cases, non-melanoma skin cancer with 1.2 million cases, and stomach cancer with 1.09 million cases [2]. The type of cancer focused on by the Bomsztyk lab is glioblastoma, a type of brain cancer. While not as common as other cancers, glioblastoma has very low survival rates. The Bomsztyk lab has developed novel tools for the high throughput studying of epigenetic features on DNA and RNA of cancer and tumor samples. These tools can be used to study a wide range of cancers and this thesis project aims to improve the efficiency of these research methods [3].

Epigenetic research is focused on lasting changes in gene expression that are not associated with DNA sequence alterations, and aberrant epigenetic changes are involved in cancer origins and progression. The Bomsztyk lab developed the PIXUL-Matrix-ChIP platform for high-throughput analysis of epigenetic processes which is based on chromatin immunoprecipitation assays (ChIP). The Bomsztyk lab and collaborators have published two main papers about ChIP methods, one in 2008 and another in 2019 [4, 3]. The first paper highlighted the usefulness of Matrix-ChIP assays for the in-depth studying of complex epigenetic events. At the time ChIP was commonly done in test tubes which limited the simplicity and throughput of the genomic studies done. Matrix-ChIP is simpler because all steps are done in the same microplate wells without needing to transfer reagents and materials between test tubes. Other advantages include “very simple sample handling, high throughput, improved sensitivity and reproducibility, and potential for automation” [3]. The system allows for 96-240 ChIP assays to be done in one day. In that paper, high-binding capacity 96-well microplates were used [4]. While these plates performed well and are commonly used in enzyme-sensitive immunosorbent assays, the nonspecific binding and background signal was higher in Matrix-ChIP than in ChIP. A better plate preparation method could save on costs since precoated plates can be expensive [3]. The second paper published by the lab discussed the PIXUL technology developed in the

Bomsztyk lab which can be used for sample preparation and chromatin fragmentation. PIXUL is an instrument that utilizes an array of ultrasound transducers to shear samples in 96-well microplates. PIXUL integration with Matrix-ChIP improves upon bottlenecks in sample preparation and chromatin fragmentation. PIXUL also allows for 96 samples to be analyzed through ChIP in less than a day [4]. Polypropylene 96-well plates are used for their cost-effectiveness and heat resistance and are protein A-coated for binding [4].

Fig. 1. This is an image of the PIXUL lab bench sonicator developed by the Bomsztyk lab and produced by Matchstick Technologies. 96 well polypropylene plates can allow for simultaneous sonication of 96 different samples at the same rate and sonication level.

This technology can be used with fresh or frozen tissue specimens as well as with formalin-fixed paraffin-embedded (FFPE) samples [5], that are widely available for cancer studies. With FFPE samples that are strongly fixed with formaldehyde, the signal sensitivity of the ChIP assay is limited by a low immunoprecipitation yield under the current lab protocol [6]. ChIP is performed in 96-well polypropylene (PP) plates which are treated with UV for 48 hrs to enable absorption of precipitating antibodies to the walls of the wells. Attached antibodies can then selectively bind and immunocapture chromatin (protein-coated DNA structure found in the cell nucleus). To solubilize chromatin from FFPE samples, it needs to be fragmented to small-size DNA-protein complexes. This is most often done using ultrasound treatment of samples. The PIXUL instrument is a 96-well plate sonicator used to fragment macromolecules such as DNA, RNA, and chromatin. With increased antibody binding capacity, formalin-fixed paraffin-embedded samples can be more successfully used for epigenetic research making a large number of samples able to be studied with high reliability and efficiency [7].

A capstone project in the Bomsztyk lab in 2019 investigated chemical etching methods to improve the antibody-binding capacity of the polypropylene plates for immunoprecipitation. The optimal solution for etching was found by testing various chemicals and measuring the surface

roughness and immunocapture in Matrix-ChIP assays, to compare UV-treated plates with chemical etching-treated plates. It was found that a sulfuric acid solution provided the best results for increasing antibody binding efficiency and immunocapture. The etched plates showed an average increase in binding efficiency of approximately 50% over the untreated plates. The cost, simplicity, and time met the goals for this procedure with it taking less than an hour to etch the plates. The downstream effects of the chemical etching on the immunoprecipitation efficiency were found to be minimal [8]. While the chemical etching method did show some promise for improving the antibody binding capacity, further exploration of plate treatment methods and how to analyze them was necessary especially to further reduce treatment time.

The UV light treatment method of activating Matrix-ChIP 96-well plates generally works well but is not sensitive enough for some chromatin proteins [7]. A common phenomenon observable to the eye is that plastics like PP turn yellow when exposed to UV light and PP surfaces can become very rough, even becoming brittle and developing large cracks. This same phenomenon of yellowing plastic is observed in the PP plates and discs treated with UV light using the protocol developed in the Bomsztyk lab. Pilot experiments with plasma etching on the other hand did not cause yellowing of the plastic and no brittleness and cracking of the plastic has been observed. These initial differences in observable qualities of the treatments highlighted the importance of surface analysis for this project beyond the surface roughness of the previous project.

This thesis aims to improve the immunoprecipitation yield of the assays by modifying the plate preparation method. The PP plates can receive an alternate treatment with radiofrequency plasma which can activate the PP surface and potentially increase the binding capacity for the ChIP antibody. A previous capstone project sought to achieve this goal through chemical etching of the plate wells which saw some improvement in yield for a limited selection of antibodies and chromatin samples compared to untreated plates. In this project, to activate 96-well PP plates we used reactive ion etching (RIE) hoping that antibody binding efficiency would increase over that of UV-treated and chemically treated PP with further improvements in reduced time and removing the need for chemicals.

Development of Design specifications:

Variations of RIE plasma treatment:

There are several parameters with oxygen etching in the RIE reactor that can be modified to achieve different qualities in the surface treatment of PP. The basis for the etch treatment recipe was the basic oxygen etch to clean the chamber as suggested by Dr. Mark Morgan, the Etch engineer at the Washington Nanofabrication facility in Fluke Hall, who assisted with determining the etch treatment design. A simple parameter to test was the treatment time of the

plates. With the generic oxygen etching being five minutes to clean the chamber that was used as the upper range of treatment limitations. This matched published etch times investigating the qualities of ion-etched plastic [9]. One and three minutes were chosen to treat PP. Choosing these time points offers the benefit of getting data at two ends of the spectrum so that macro trends between the treatments can be investigated as opposed to minor differences between similar time points. Initially, two-minute RIE-treated plates were planned as well at first, but preliminary data showed that it was not significantly different from the other two permutations. This saved time and resources carrying out lengthy ChIP experiments. The one-minute treatment can represent the qualities of shorter treatments and the three-minute treatment can represent the qualities of treatments longer than one minute.

Fig. 2. Closeup picture of 96 well sample plates used in ChIP and with PIXUL highlighting the conical shape of the wells [10].

The next important parameter to consider is the power setting of the reactor. The reactor can range from 10 to 300 watts in power and 50 watts is used for the standard chamber clean recipe. Increasing the power of the etching instrument correlates to the plasma cloud of the reactor being more energized and leading to more charged particles potentially activating the surface. However, too much power can lead to unintended consequences. To create another binary for comparison the two different treatments were tested with PP plates at 50 watts and 150 watts. 50 watts was the baseline power for the chamber clean cycle so that was used as the low end of the spectrum and 150 watts was chosen as a midway point of the available power and as the upper end of the variable. These treatments used three minutes for the treatment time so that the permutations of power settings could be standardized to the original timepoint treatment variation. Only one variable was changed between experiments with different parameters of the etch treatments. Another parameter investigated was chamber pressure which could range from

10 to 200 mtorr. The two points chosen for this parameter were 150 mtorr for high pressure and 50 mtorr for low pressure. 150 was chosen as the base pressure because higher pressure should increase ion scattering so the sides of the wells of the plate would have more surface activation because the more densely populated chamber will cause more lateral trajectories of ions through collisions [11]. The standard ChIP protocol is to have 50 uL of chromatin solution in the wells so approximately only the bottom fifth of the wells need to be activated which is still on the sloped portion of the wells but moderate scattering would likely be beneficial to guarantee full well coverage **(Fig. 2)**. The final parameter investigated was the oxygen gas flow rate which determined the speed and volume of oxygen gas let into the chamber to fuel the plasma cloud and bombard the plate. The gas flow can range from 10 to 100 standard cubic centimeters per minute (sccm). The standard oxygen for each treatment of 60 sccm was chosen because it is approximately the midpoint of the range. The high oxygen was chosen as 100 sccm to see the broadest spread of the range to get a trend and going lower than 60 would likely cause little activation since that is the active gas in the plasma.

Treatment Permutation:	Pressure (mtorr)	RF (Watts)	Step time (min)	O2 Gas flow (sccm)
1 min	150	150	1	60
3 min	150	150	3	60
Low Power: 50 Watts	150	50	3	60
Low Pressure: 50 mtorr	50	150	3	60
UV + Plasma	150	150	3	60
High Oxygen: 100 sccm	150	150	3	100
UV control	N/A	N/A	48 hours	N/A

Table 1. This table shows which treatment variables change for each experiment and the baseline values throughout the experiments.

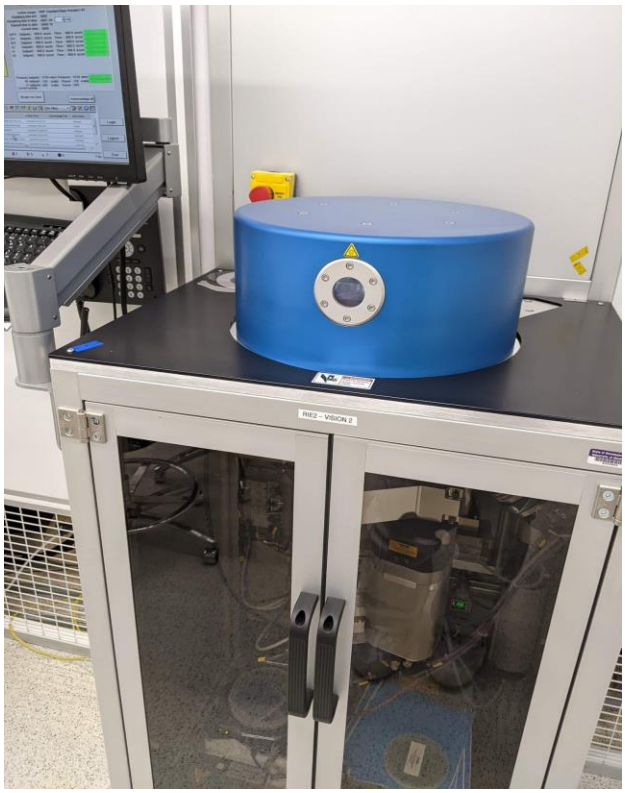

Fig. 3. Imaged above is the RIE reactor at WNF in Fluke Hall. The chamber where materials are placed in the blue circular container at the top. The container simply lifts and as many as four microplates can be placed inside. Inside the glass chamber, many devices and components are contained like vacuum pumps, gauges, and gas supply lines. In the top left of the image, the computer screen interface can be seen which is how the reactor is operated.

An important consideration of the plasma treatment design specifications is the cost, effort, and time to do the treatment on the plates. It costs 77 dollars an hour to rent the RIE machine. Therefore, if the three-minute treatment method is used, four plates could be put in at a time and at least two batches of plates could be run within 15 minutes of renting the machine which includes chamber vent and pressurizing times. This means that it would cost 2.40$ per plate to do plasma treatments on the polypropylene plates. A rough estimate of less than 5$ per plate was the original design specification for cost, but this was always dependent on plate performance. This can be compared to UV light treatment. The UV light setup in the Bomsztyk lab is free to use, but the plates need to be treated for 48 hours to activate the plates evenly. The plasma treatment occurring in less than an hour is one good aspect of the method. UV light is low effort and essentially free, but plasma treatment is not much more expensive and majorly saves on time, so experiments do not need to be delayed waiting on plates. Overall, the key metric of the treatment method's success is the increase in antibody binding capacity and immunoprecipitation yield.

BCIP/NBT dye substrate system:

Protein A is a protein discovered in the bacteria Staphylococcus aureus and can respond to DNA topology. Polypropylene discs and microplates can be treated with protein A to immobilize protein A on the surface of the materials. Polypropylene is sensitive to the binding of protein A and this capacity can be increased if the surface is chemically activated. Protein A allows for various antibodies like Pol II or IgG to attach to the protein A structure and therefore also be used to immunocapture proteins of interest to the polypropylene surface.

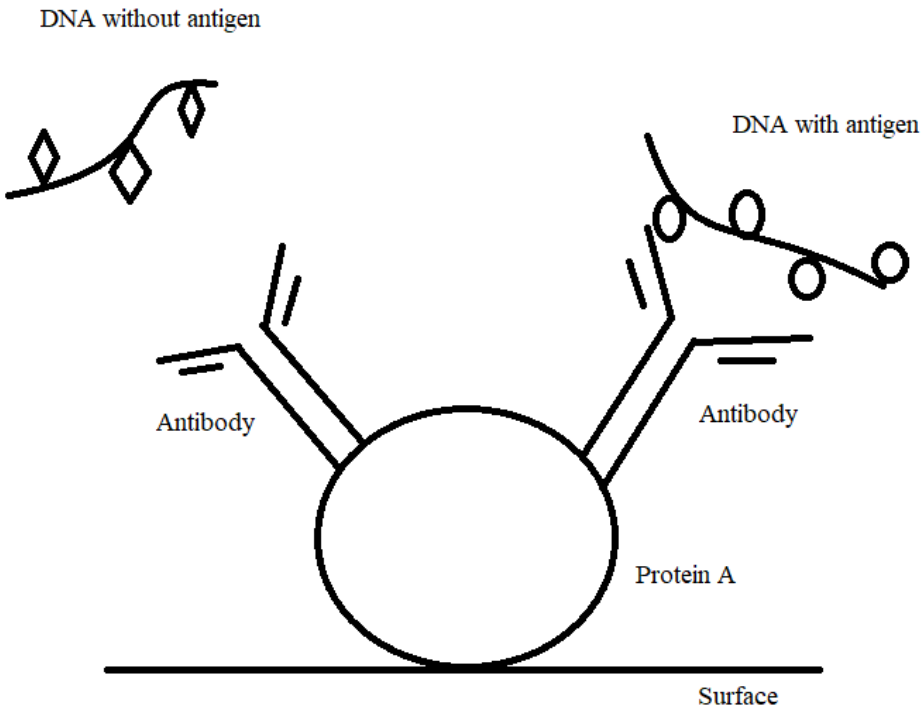

Fig. 4. Shows a cartoon depiction of the process of immunocapture by which protein A attaches to a plastic surface, antibodies then attach to protein A which can then selectively bind chromatin based on which antigens (proteins) are present on the chromatin (a complex of DNA and proteins found in the nucleus).

One key metric to determine the viability of RIE plasma treatment on polypropylene plates for ChIP was to treat polypropylene discs decorated with protein A bound with an alkaline phosphatase-conjugated antibody with its BCIP/NBT (5-bromo-4-chloro-3-indolyl-phosphate /nitro blue tetrazolium) substrate and dye them. It was known from previous lab experiments that UV light-treated polypropylene using alkaline phosphatase-conjugated antibody bound to protein A did respond to the substrate dye system. This means that the UV light-treated polypropylene would then have protein A attached to the plastic surface after 20-60 minutes of incubating in a protein A solution on a shaker table. Then an alkaline phosphatase-conjugated antibody could be attached to the plastic surface after 20-60 minutes of incubation followed by the BCIP/NBT substrate dye. The immobilized dye substrate would remain attached to the surface with multiple

washes. As such, this method serves as a metric for surface binding capacity. For example, plates not treated with UV light were not dyed by the substrate system.

I carried out these experiments on polypropylene discs for a side-by-side comparison of UV light treatment vs. plasma ion treatment. Untreated discs were used as a controlled trial along with other control trials as detailed below in the Materials and Methods section. This metric is key to determining the viability of plasma-treated plates because if the discs are not dyed after the procedure and UV light-treated plates are dyed, then that would mean that plasma light would not be activating the surface of the plastic sufficiently to bind the protein A molecule or bind the antibody to protein A attached to the wall. This would result in no dye being left on the plastic surface after the dye was washed away.

Despite the lack of quantitative data, the dye being present in similar quantities to UV light-treated discs is an obvious metric of the viability of RIE treatments on increasing surface roughness and activation of polypropylene plastic. This dye experiment was only meant to test the surface modification of the plastic from plasma treatment as a proof of concept. This surface analysis sufficiently determined whether the plastic surface was modified by UV light treatment or plasma treatment when compared to the control plastic discs.

Water Contact Angle (WCA):

As more ChIP experiments were completed in the early stages of the thesis project it became clearer that surface chemistry and qualities would need to be investigated to get a clear picture of how etching treatment impacts the materials signal performance in ChIP assays. An important surface analysis method for determining indicators of antibody binding capacity of treated polypropylene surfaces is water contact angle measurements. WCA measurements involve placing a droplet on the surface of a material which can be done parallel to the ground so that the droplet does not drift with gravity, there are instruments like goniometers that use mechanized angled surfaces to electronically record WCA measurements. The angle between the surface of the material and the upper angle of the droplet where the corner of the droplet and the surface meet is the WCA. This value measured in degrees is a measurement that reflects the hydrophilicity of the surface.

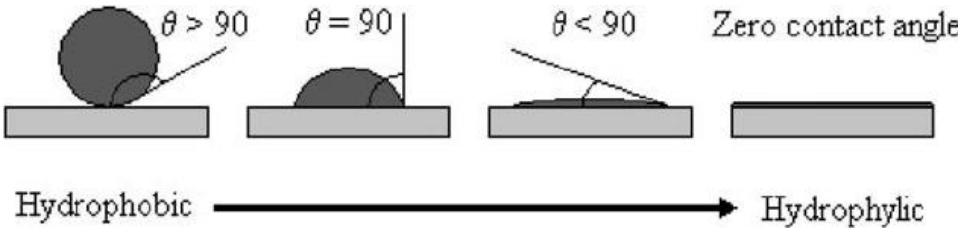

Fig. 5. This figure shows the categories for different levels of hydrophilicity and how they are determined. At WCA measurements of over 90 degrees, the surface is considered hydrophobic or approaching super-hydrophobicity.

Below 90 degrees the surface is defined as hydrophilic and as the WCA approaches 0 the surface is considered super hydrophilic [12].

The more that a surface is hydrophilic, often oxygen-rich and or highly polar areas of atomic charge, the more surface adhesion forces a droplet to collapse. Specifically, these surface adhesion forces partially counteract the water tension forces within the droplet which lets the droplet spread out over the surface of the material. As the droplet spreads out more the angle of the WCA will decrease reflecting the higher hydrophilicity of the surface. Any measurement between 10 and 90 degrees can be considered a hydrophilic surface. Anything above 90 degrees is considered hydrophobic and can approach super hydrophobic angles above 150 degrees with a surface chemistry that is more nonpolar. Below 10 degrees the measurement approaches zero contact angle and becomes super hydrophilic.

The WCA measurements are extremely helpful assays as they can be done rapidly and cheaply allowing for high throughput of feedback on chemical changes to surface wettability with the sessile drop method as further detailed in the methods section. There are potential errors and variability in the degrees of the WCA measurements due to imperfect measurement techniques without access to a goniometer. Still, this variability can be addressed by increasing the number of repeated WCA measurements and surface sample replicates. Changes in the angle measurement can be partially attributed to user variation through the interface of the software used to optically measure the droplet angle interface. These variations do not exceed 1-3 degrees which are similar levels of variation reported in regular WCA experiments. Importantly, the degree values provide quantitative data on surface wettability and therefore treatment performance measured by WCA is an impactful quantitative assay along with the ChIP assays and other surface analysis assays.

XPS Chemical Survey:

XPS is the most popular and widely used technique for analyzing the surface chemistry of a material. This method can measure the chemical and even electrical states of the surface atoms on a material providing a spectrum. XPS works by using X-ray beams to irradiate a solid surface within a chamber, the irradiated surface then releases electrons with specific kinetic energy. These photo-electron emissions can then be focused and measured through an electron spectrometer which counts the electrons and measures their individual kinetic energies. These measurements can then be represented as a spectrum of electrons counted as time passes and binding energy (BE) as the kinetic energy of the electrons corresponds to the BE of the irradiated atomic bond. BE is calculated from the equation: BE = x-ray energy – kinetic energy. If the survey produces a peak at 530 eV, then that would represent atomic oxygen on the surface, with the photoelectrons from the oxygen having on average a ~530 eV BE.

The importance of XPS as a surface analysis tool in this project is that it can quantify the chemical properties of UV and plasma-treated PP discs that relate to hydrophilicity and antibody

binding capacity in ChIP. The chemical species targeted were general carbon and oxygen species with the XPS survey plot. The XPS survey shows a plot with the number of and BE of electrons from the surface of the sample. The high-resolution (hi-res) scan of individual elemental peaks shows a similar plot of measured electrons and their energy which is then used for fitting peaks to the overall curve. These peaks can correspond to different chemical species like hydrocarbons (C-C/C-OH) carboxylic acid (C-O-H), carbonyl (C=O), and carboxyl groups (O-C=O). These species were chosen to represent a scale of polarity and molecular charge between the species. C-C has the lowest dipole charge, and O-C=O has the most negative dipole charge in that order. Theoretically, more of the highly negative species leads to more surface wettability. Both the XPS survey and hi-res measurements were important so that the impact of surface oxygen content versus the type of oxygens present could be compared.

Profilometer Surface Roughness:

The importance of measuring the surface roughness of treated PP for this project is that etching treatments should increase surface roughness increasing surface area. More surface area should increase the number of proteins that can bind therefore increasing antibody binding capacity and subsequently ChIP max signal. Determining the best way to measure roughness with the profilometer was challenging and involved several iterations of data collection and analysis methods. One consideration was that the PP sheet had a rough side and then a glossy smooth side, originally the rough side of the discs were tested. These measurements produced plots with very large changes in surface height on the order of thousands of nanometers. Even to the eye, there was not much discernable difference in the roughness of the surface traces between UV, plasma, and untreated discs. Calculations of average roughness and coefficient of variation revealed there was no discernable difference in roughness between etching treated discs and untreated discs.

The most glaring issue with analyzing the rough side of the disc is that the untreated discs already had large amounts of perceived surface roughness with changes in height on the order of thousands of nanometers like the other plots. The glossy side of the PP discs on the other hand seemed more conducive to measuring roughness in this manner. Profilometer measurements revealed that the glossy side was much closer to uniform height before treatment with variations being in the hundreds of nanometers. More surface profile plots were obtained for 1- and 3-min plasma, and UV-treated discs on the glossy side which seemed to better reflect surface roughness features both observationally and analytically. While the glossy side did have benefits, the natural curve of the discs was still complicating the analysis of the plots and was more pronounced on the glossy side because overall changes in height were less throughout the plots. This curvature could not be removed as the discs were not naturally flat and discs became less flat due to treatment and over time to the naked eye. More trial and error were needed with the analysis side after the data collection, the two main methods of analysis then pursued were a calculation of average surface roughness and coefficient of variation of individual plots.

The method of roughness data collection by way of a profilometer was determined through trial and error. One aim of the measurements was maximizing the trace distance so a wider range of the roughness features could be viewed within the trace and encompass some of the larger features that might be present. However, as trace distance increases the curve of the disc becomes more of an issue, so the trace is less accurate of surface height parallel to the disc. This issue seemed to be more impactful than the surface height between peaks and valleys starting at trace distances over 1 mm which was the chosen trace distance. This curvature that does remain can be remedied by leveling the data after the trace has been taken. To attempt to get a good estimate of the average roughness caused by the treatments, multiple locations were treated on each disc but kept in the same orientation for each replicate and treatment tested. The data collected represents N=6 with three locations measured on each disc and two-disc replicates included in the data in the report section. The locations tested were at the center of the disc, 2 mm to the left of the center, and 2 mm above the center of the disc.

Quantitative ChIP experiments:

Ultimately the key benchmark in this thesis project is the ChIP data which can be used quantitatively to determine how effective RIE treatments are at activating the surfaces of the PP plates and therefore how effective the treatments are at immunoprecipitating chromatin samples compared to UV light. It was important that these quantitative data measurements were made side by side to account for contamination and error. To this end, I performed sets of ChIP experiments with one UV-treated plate and one permutation of plasma plate so that each experiment could be compared to the UV-standard results.

To further increase the reliability of the data acquired from these quantitative experiments, triplicate chromatin samples were used. Briefly, serum solution was used to treat serum-starved colon cancer cell line HCT-116 cells in 96-well plates to obtain the chromatin samples. Treatment of these cell cultures with 10% fetal bovine serum (FBS) can activate the expression of a group of genes which can be detected by the increased recruitment of RNA polymerase II (Pol II) [8]. I used chromatin from these cells treated with 10% FBS for 0, 5, 15, and 30 minutes which activates the expression of early response genes like EGR1. After serum treatment, cells were cross-linked with formaldehyde (this ensures that the chromatin proteins remain bound to DNA) in a lysis buffer and then treated with ultrasound in PIXUL. This resulted in a 96-well microplate with sheared chromatin in every well [8].

The EGR1 gene is a transcription master regulator that controls other genes and plays a key role in response to growth factors and DNA damage. Three sites of the EGR1 gene were targeted in these ChIP experiments: the intragenic region 15kb upstream of the EGR1 gene, the exon 1 site, and the exon 2 site within the coding region of the gene. The -15kb site was used as a negative control for the Pol II (50 ul/ml PBS) antibody with expected low levels of immunocapture yield. Exon 1 (close to the transcription start site) and exon 2 sites were chosen

as positive controls and expected to see a high response at some time points from serum-treated HCT-116 cells. The inverse is true for the CTCF insulator factor recruitment (10 ul/ml PBS), where it should have a good signal at -15kb but low at the two exon sites. [8]. Histone H3 (20 ul/ml PBS) is a component of the nucleosome and decorates the entire gene. Thus, I used the H3 antibody as a positive baseline that should be approximately the same across all sites. The mouse non-immune IgG antibody (40 ul/ml PBS) is used as a negative control since very little chromatin should be captured with a non-specific antibody.

Materials and Methods:

Plate preparation protocol:

Bomsztyk lab has developed protocols for the UV light treatment of 96-well polypropylene plates. This involved taking polypropylene plates directly out of their boxes and leaving them underneath a UV light for approximately 48 hours. After UV treatment, plates are washed with a phosphate-buffered saline solution (PBS: 137 mM NaCl, 10 mM Phosphate, 2.7 mM KCl, pH 7.4), and 100 uL of PBS containing 0.2 μg of protein A is added to each well. Protein A is allowed to bind to the wall wells by shaking the plates (means for efficient mixing) for 24 hours at room temperature. 96-well plates with protein A-loaded wells can be stored in a refrigerator for at least several days and then be used for ChIP assays.

This process was only slightly modified for plasma-treated plate generation. The plates were taken to the RIE reactor at the WNF facility in a sealed bag. The plates were then placed inside the vented chamber of the RIE reactor. This chamber was then pumped down to a 1E-7 torr vacuum for the recipe to run. The basic plasma treatment used 150 mtorr pressure, 60 sccm oxygen flow, and 150 watts for power with a 1 or 3-minute treatment time. Once the procedure was completed the chamber was vented, plates were marked, and returned to the sealed bag. Minimal exposure to open air, as well as air particulates, was a priority to make sure that the effects of the plasma treatment were not compromised while taking the plates back to the Bomsztyk lab. Within 40 minutes of plasma treatment, the plates were washed with PBS and incubated for 24 hours with 100 uL of the protein A-PBS solution as with the UV protocol.

BCIP/NBT dye substrate system:

The polypropylene discs underwent the same 1- or 3-minute plasma treatments as described above. These discs were then submerged in the protein A solution for 30 minutes (30 minutes was determined as sufficient exposure because no noticeable difference in dye coloration was observed between 30-minute incubation vs. 24-hour incubation). Then the discs were submerged and incubated with 40 uL alkaline phosphatase-conjugated anti-rabbit antibody solution with every 1 ml of PBS for another 30 min. The discs were then left in 20 uL of a 1:1:8

ratio of BCIP dye solution (yellow in color): NBT dye solution (blue in color): PBS for 10 minutes. The BCIP/NBT substrates react with alkaline phosphatase to generate precipitated dye and leave the surface of the discs stained with blue/purple color. After each of the three incubation steps, the discs were washed with PBS twice for five minutes.

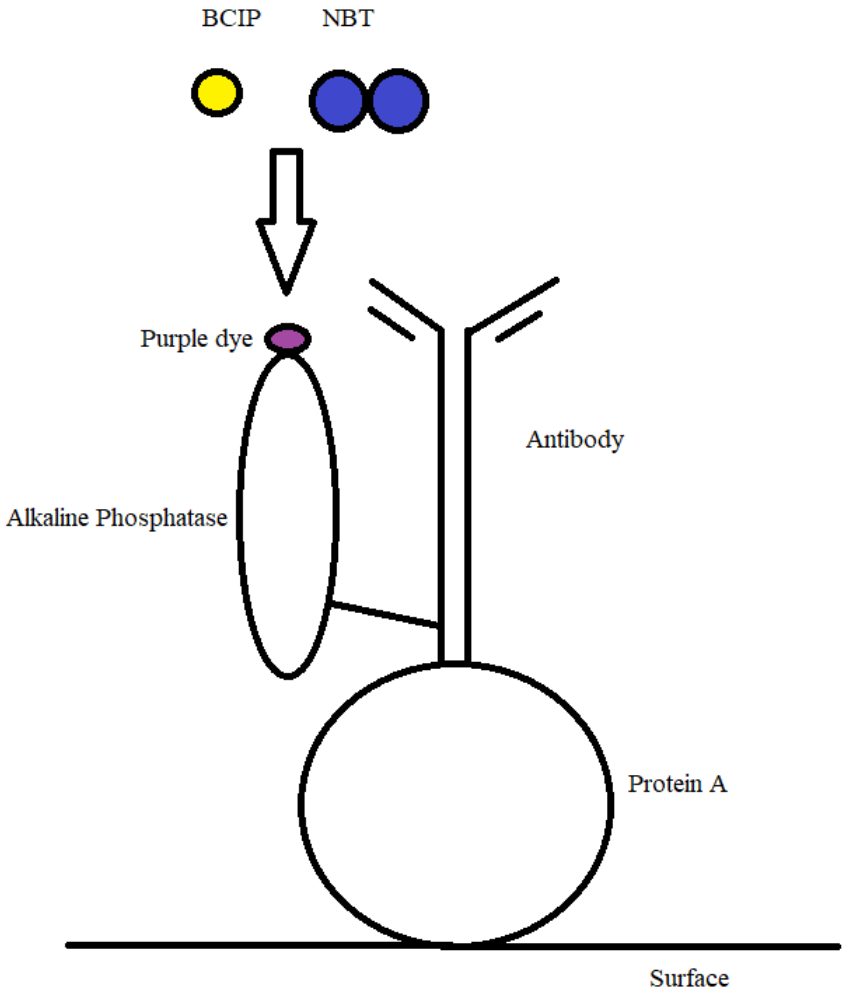

Fig. 6. Shows the process of BCIP and NBT reacting with alkaline phosphatase to form a purple-colored dye. This dye reaction is used to measure protein A and antibody absorption that happens to the treated surface since the phosphatase is connected to the antibody that attaches to protein A.

The premise is that protein A attaches to the UV light and plasma-treated discs much better than to the untreated discs. The next premise was that the antibodies would only attach to plasma and UV-treated plates that had also been treated with protein A. The final premise **(Fig. 6)** was that only treated discs with protein A and bound antibody conjugated to the alkaline phosphatase will react with the BCIP/NBT substrates and generate the dye color on the surface. To test all the permutations, negative controls for each stage of treatment were included at later

stages. For example, one treatment would be a 3-minute plasma treatment, negative for protein A treatment, and positive for antibody treatment. This example tested whether the antibody was binding to only protein A or was binding to the discs independent of protein A. While the negative controls were useful, the data from these experiments were only qualitative, and therefore this experiment was used as a proof of concept for the development of plasma-treated, and UV light-treated 96-well plates.

Water Contact Angle:

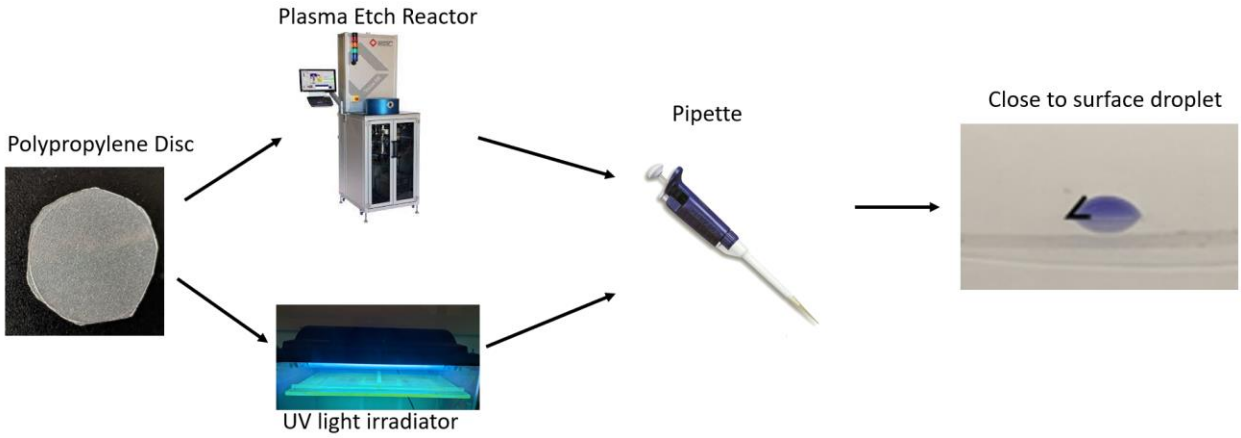

Fig. 7. Shows the procedure for measuring the WCA. First, the PP discs were cut and then treated with plasma or UV etching. A standard pipette is then used to add droplets of dyed water to the surface. The final panel then shows the photo of the WCA measurement along with the angle measurement tool from the software used to optically make the measurements.

For the WCA assay, PP discs were cut and then taken to their respective treatment with UV light or RIE plasma etching. After treatment, these discs were tested within an hour to minimize the atmospheric loss of surface chemistry and qualities from the treatment. The WCA measurements were completed with a flat surface placed drop method where distilled water in a small volume is formed into a droplet and lowered onto the sample surface [13]. For this project, the method was replicated by using a 10 uL pipette to form a 5 uL droplet at the end of the pipette. The droplet was composed of distilled water mixed with a 1:100 ratio of bromophenol blue dye to assist with viewing the droplet without affecting the chemistry of the water.

The 5 uL droplet was lowered from the pipette onto the disc surface minimizing the effect of the pipette on the structure and formation of the droplet on the surface interface. The gas, solid, and water interface at the corner of the droplet is formed and then can be measured. Images were taken immediately after the droplet was formed on the treated surface with a smartphone camera lowered to approach the angle of the plane of the surface and droplet. Image analysis was then done with the angle measurement feature with ImageJ software. Angle measurements were done with thin yellow lines for more accurate optical measurement of the

droplet contact angle, lines were later replaced with larger black lines for ease of figure viewing **(Fig. 16)**. The treatments selected for initial surface analysis experiments were untreated, UV light treated, 1-minute and 3-minute plasma treatments and were done in triplicates.

XPS Chemical Survey:

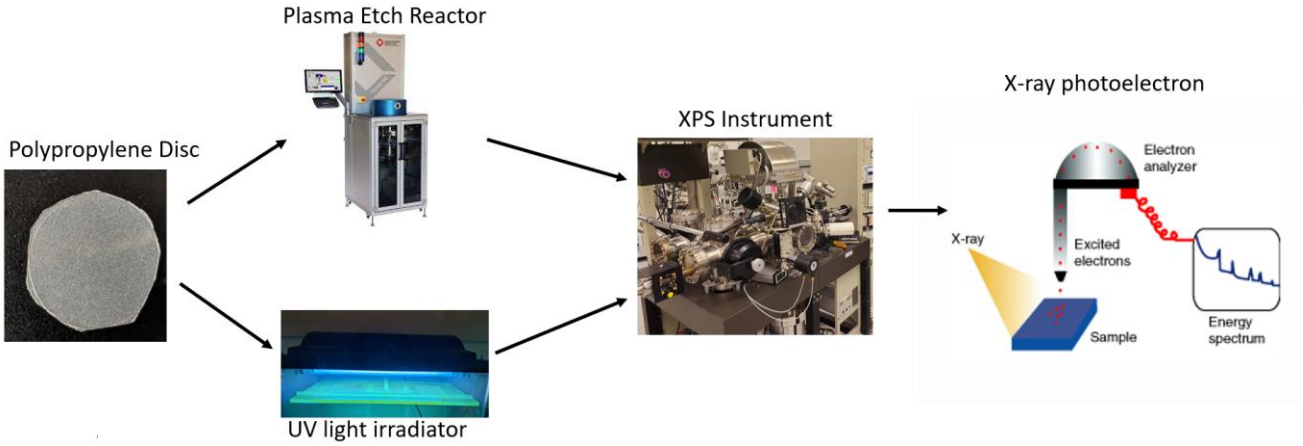

Fig. 8. Shows the process of XPS measurements by taking PP discs through etching treatment then to be measured through XPS and the final graphic shows a representation of XPS taking place. The sample area is shown to be irradiated and how electron energies are measured and put into a survey spectrum. Below the final image is a representation of the four sets of chemical species targeted by the four curves within the hi-res spectrum as well as the polarity of those molecules.

After treatment, PP discs were wrapped in aluminum foil to prevent contamination during transport to the Molecular Analysis Facility on the UW campus for XPS and the profilometer measurements. The operation of the XPS instruments and collection of data was handled by Dr. Samantha Young, the XPS faculty expert. The two spectra taken were the standard XPS survey and the high-resolution spectra scan for carbon and oxygen. All XPS spectra were taken on a Surface Science Instruments S-Probe spectrometer. This instrument has a monochromatized Al x-ray source and a low-energy electron flood gun for charge neutralization. The X-ray spot size for these acquisitions was 800 x 800 μm. All samples were run as insulators. Pressure in the analytical chamber during spectral acquisition was about 5 x 10-9 Torr. The pass energy for survey spectra (composition) was 150 eV. The pass energy for high-resolution spectra was 50 eV. For the high-resolution spectra, all binding energies were referenced to the C ls C-C bonds at 285.0 eV. Data analysis was carried out using the Service Physics Hawk Analysis 7 program (Service Physics, Bend OR) and CasaXPS.

Profilometer Surface Roughness:

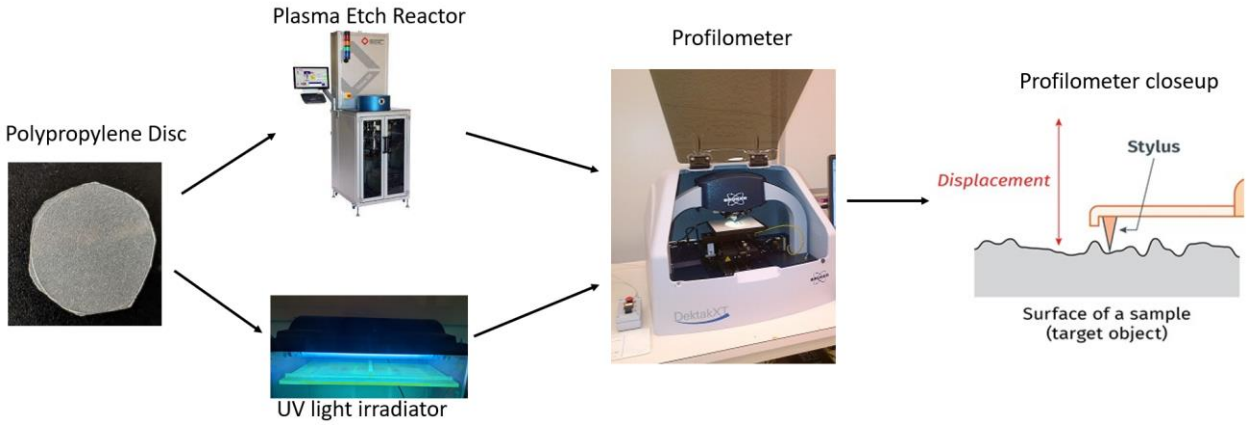

Fig. 9. Shows the process of measuring the roughness of PP discs where the discs are UV or plasma etched and then placed on the platform of the profilometer. The last panel is a graphic depicting the mechanism by which the surface trace of the profilometer is measured by dragging a fine stylus of the surface of the sample.

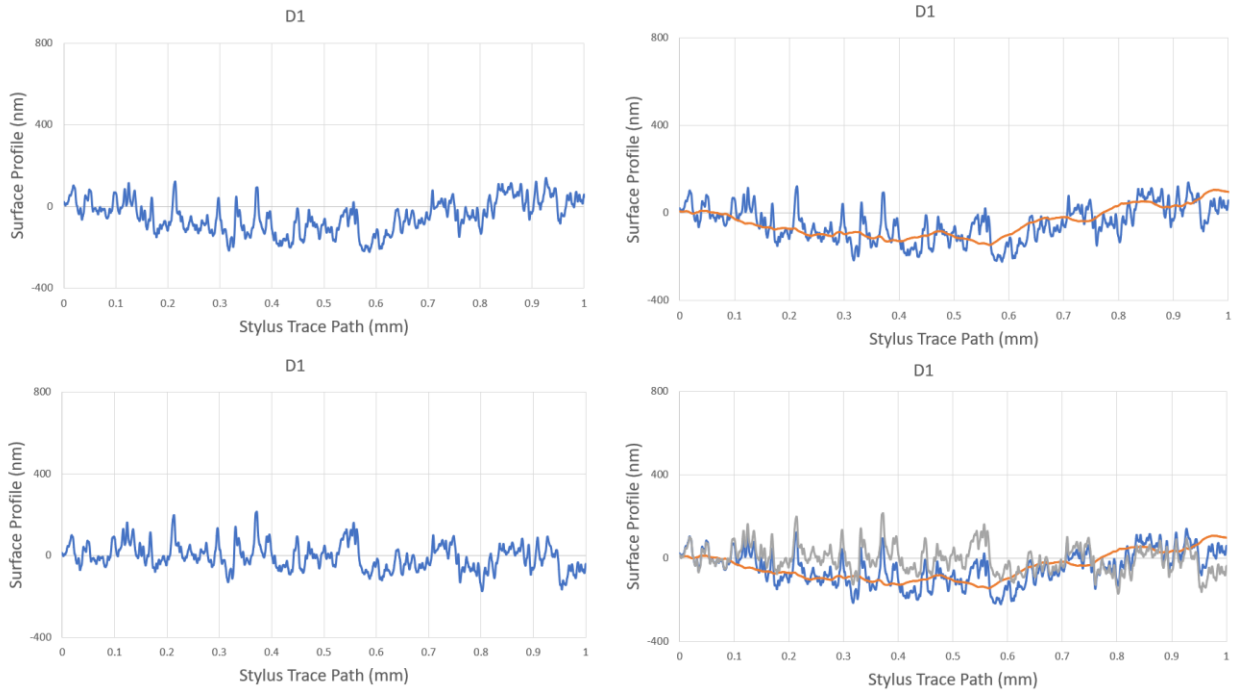

Fig. 10. shows the process of leveling the profilometer trace for an untreated disc location. The top left surface trace shows the direct output of height recorded by the stylus of the machine. The top right plot shows the original trace with the approximation curve used for leveling. The bottom left plot shows the leveled trace after the approximation curve was applied. The bottom right plot shows the original trace, approximation curve, and leveled surface trace.

The **Fig. 10** shows the process used for leveling the data received from the profilometer trace of one location on one disc which was repeated for each replicate and the other treatments. The surface approximation curve used to estimate the midpoint or surface height of the disc is made from an average of the 500 adjacent points from the trace which is made up of 6000 points. This corresponds to approximately 83 microns length used for each point of the average. The approximation curve at each point was then subtracted from the data value at that point to achieve leveling. In this example, the middle of the plot raises and the sides lower to help remedy the macro scale curve of the disc so that the frame of the average of the trace follows closer to the true parallel plane of the curved disc. Some discs had larger macro curve features than others which could be easily seen with the eye and were more pronounced in UV-treated discs and as days after treatment, so discs were measured within 2 hours of treatment.

The following is a common roughness formula that is used to calculate average roughness for the profilometer traces in this paper: Ra = 1/n * SUM(ABS[Zi-Zmean] [14]. In the equation, Zi correlates to the points along the leveled trace of the surface while Zmean is the average value of the trace which is also the average height of the surface. The metric is the summation of the absolute value of the difference between each point on the trace and the average value of the trace. The total summation is then divided by the number of data points within the trace with the 1/n term. This equation essentially gives a measure of the variation of the surface through the peaks and valleys of the surface based on the average height of the surface. This works much better with the leveled data since the unlevelled data would put the mean above many peaks in the center of the plot and below many peaks at the sides of the plot. With the data leveled the mean for the roughness equation intersects many of the peaks and is close to zero which more accurately represents a flat disc as opposed to a curved disc at the macro scale.

Quantitative ChIP experiments:

The protein A loaded 96-well plates Matrix ChIP plate **(Fig. 2)** are washed with PBS and then treated with blocking buffer (60 min at RT) to minimize non-specific binding of chromatin to the wells of the plates. The blocking buffer is made from 20 mL PBS, 1 g of Bovine Serum Albumin (BSA), and 200 uL of 10 ug/uL single-stranded salmon DNA. While the Matrix ChIP plate is being blocked, 5 uL of chromatin solution is mixed with 30 uL of blocking buffer for a total of 35 uL and added to each well of the 96-well preparation plate. Then 25 uL of antibody and blocking buffer solution is added to each designated well. In these experiments, I tested Pol II antibody, H3 antibody, CTCF antibody, and mouse IgG antibody was used as a negative control antibody. The 1st 4 wells of a row contain the 4 different sonicated chromatin samples in the order of 0, 5, 15, and 30 minutes. This time series of the samples were repeated within the same row to produce triplicate data as shown in **Fig. 11**.

Series													A
A	10	1	0.1	0.01	0.001	0	10	1	0.1	0.01	0.001	0	STD
B	0.1	5.1	15.1	30.1	0.2	5.2	15.2	30.2	0.3	5.3	15.3	30.3	Input
C	0.1	5.1	15.1	30.1	0.2	5.2	15.2	30.2	0.3	5.3	15.3	30.3	Pol II CTD
D	0.1	5.1	15.1	30.1	0.2	5.2	15.2	30.2	0.3	5.3	15.3	30.3	IgG
E	0.1	5.1	15.1	30.1	0.2	5.2	15.2	30.2	0.3	5.3	15.3	30.3	H3
F	0.1	5.1	15.1	30.1	0.2	5.2	15.2	30.2	0.3	5.3	15.3	30.3	ctcf
G													
H													

Fig. 11. Shows an example of the layout for one plate experiment. The first row shows the concentration of the standards in ng/uL. The other rows show the chromatin samples labeled with the HCT116 serum-treated time series and triplicate order. The right side of the figure lists which ChIP antibody was used in each row.

The 1st (A) and 2nd (B) rows **(Fig. 11)** are used for the DNA standards and input DNA, respectively. These are added to the original ChIP plate after the incubation plate is used. The standard DNA is made from a human genomic DNA stock made in the lab, as follows 10 ng/uL, 1 ng/uL, 0.1 ng/uL, 0.01 ng/uL, 0.001 ng/uL, 0 ng/uL in the elution buffer. The input solutions are made from a mixture of 5 uL of chromatin samples and 50 uL of elution buffer (25 mM Tris base, 1 mM EDTA, pH 10) with 0.5 uL of proteinase K (10mg/ml). Rows A and B are filled in the final step of the procedure to the original ChIP plate.

Rows C-G **(Fig. 11)** are filled with 60 uL per well of buffer and the matching antibody and chromatin pair, this incubation plate is then processed for 1 hour in MatrixMate, a shaking and washing station developed by the Bomsztyk lab. The Matrix ChIP plate can then be aspirated and washed with PBS to remove the blocking buffer. At this point, 50 uL from each well of the incubation plate is added to the Matrix ChIP plate. The incubation allowed chromatin samples to bind to the antibodies. The Matrix ChIP plate with the bound chromatin samples and antibodies is then set on the MatrixMate for another hour of incubation at which time the MatrixMate washes each well three times with Immunoprecipitation buffer [150 mM NaCl, 50 mM Tris-HCl (pH 7.5), 5 mM EDTA, NP-40 (0.5%vol/vol), Triton X-100 (1.0% vol/vol), (pH 7.6)] followed by another three washes with TE buffer [10mM Tris, 1mM EDTA, pH 7.0]. After the washes are finished, the only chromatin left inside the wells of the Matrix ChIP plate should be the sheared chromatin fraction that is bound to the immunoprecipitating antibodies that are bound to the protein A immobilized to the wall of the wells. The chromatin fractions that have more of the targeted protein (e.g., Pol II) bound to a given region of DNA should be immobilized in greater quantities, which is the basis of the assay's ability to measure chromatin-bound proteins in a stretch of DNA **(Fig. 4)**.

The immobilized protein cross-linked to DNA is then removed from the sides of the wells with the elution buffer and proteinase K solution described above. The standard DNA and input DNA solutions are also added at this step to the 1st and 2nd rows, respectively. The Matrix ChIP

plate is then put in a thermal cycler where the cycler runs at 55ºC for 45 minutes and then 95ºC for 10 minutes. This process allows for the proteinase K, which digests the proteins, to free the immobilized DNA for real-time PCR (qPCR) analysis to determine the DNA concentration.

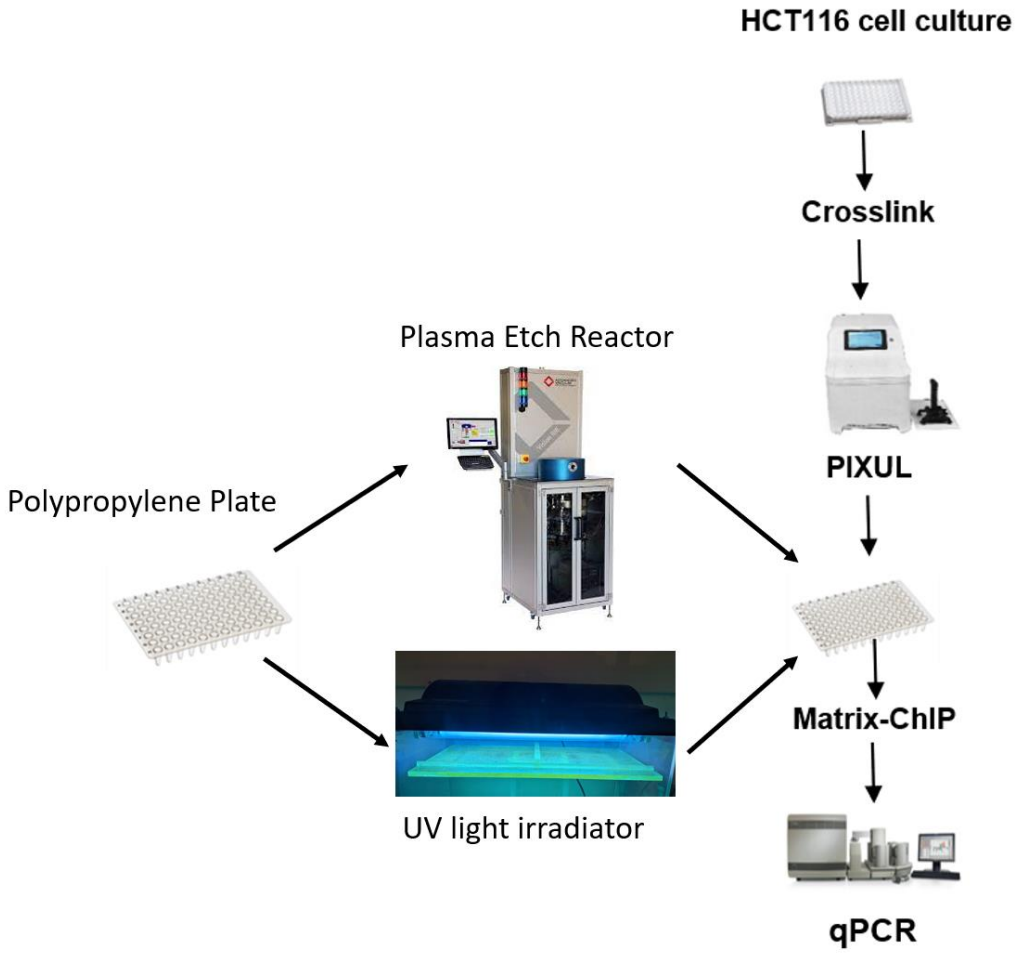

Fig. 12. Describes the workflow for obtaining qPCR data from cultured HCT 116 cells. Cells are first treated with 10% FBS. Following this treatment, the cells are sonicated in the PIXUL instrument to obtain sheared chromatin. Sheared chromatin is used in 96-well Matrix ChIP experiments [4].

Real-time PCR (qPCR) is performed in 384 well plates in the ABI7900 machine. The sequences of the primers used for this set of experiments targeted the gene sites hEGR1 were as follows:

-15kb F: GAGGCACTCTGCTCACCAAA R: GATGCCTGCGAGGATGGAAA
Exon1-5 F: AGCTCTCCAGCCTGCTCGT R: GGTAGTTGTCCATGGTGGGC
Exon2-3 F: GCTGAGCTGAGCTTCGGTTC R: TCGCCGCCTACTCAGTAGGTA

qPCR data are analyzed and plotted using the PCRCrunch Excel tools developed in the Bomsztyk lab. Chromatin concentration values for each ChIP sample are calculated from the average ct values of the qPCR data. These data plots show the fraction of ChIPed DNA compared to input DNA. The program generates a graph grid organization of chromatin values

selected and can be arranged based on settings like antibody and gene site used. The program also offers automatic significance t-tests for the samples to show the statistical relevance compared to other data points within the individual plot.

Results:

Assessment of the Antibody Immobilization on Polypropylene Discs by using NBT/BCIP dyes:

Original Disc Experiment

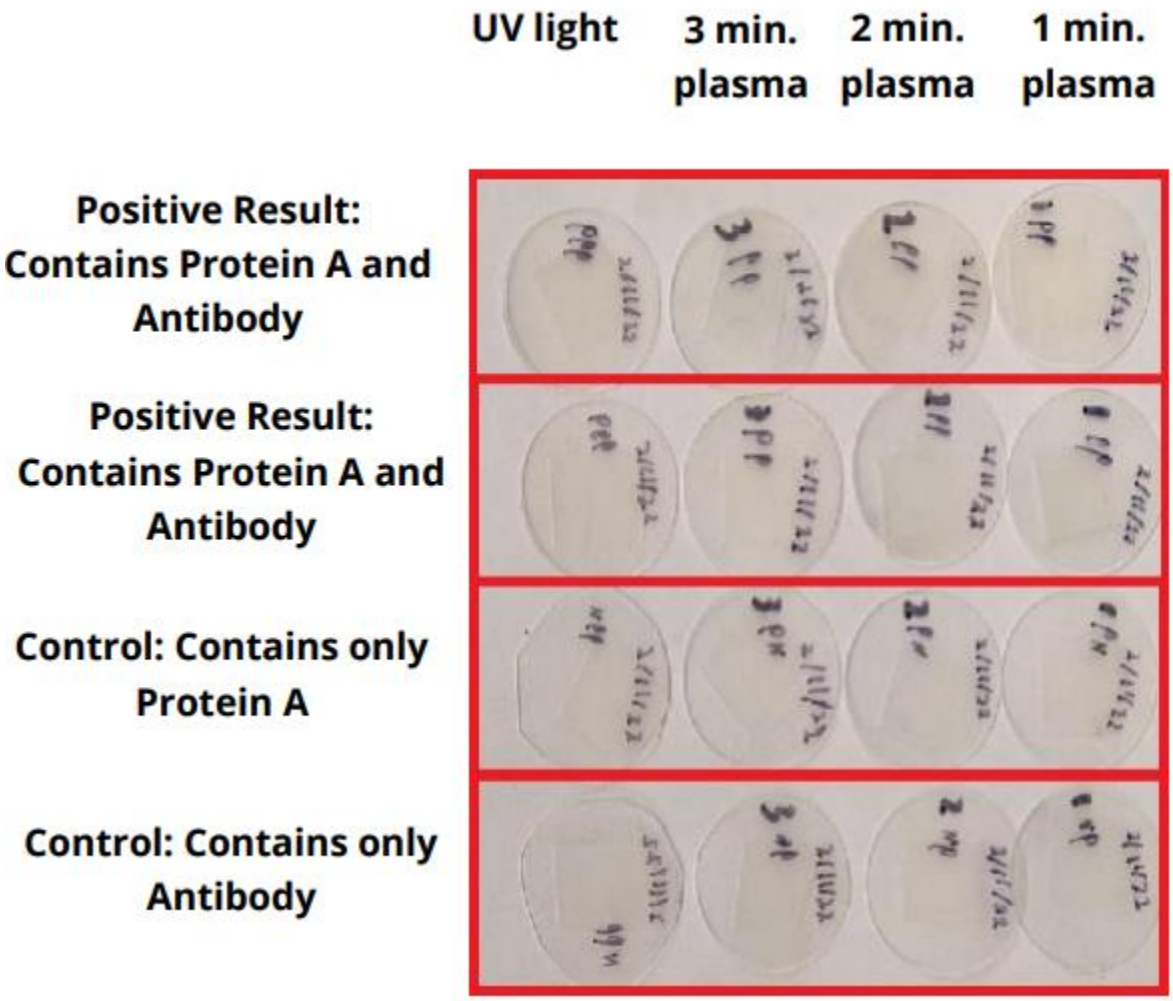

Fig. 13. All discs show little to no dye coloration except partially in the top left disc which was UV, protein A, and antibody-treated. This first experiment likely failed due to the unrefined procedure for treating the discs with protein A and antibodies.

Improved Disc Experiment with UV light and Negative Control

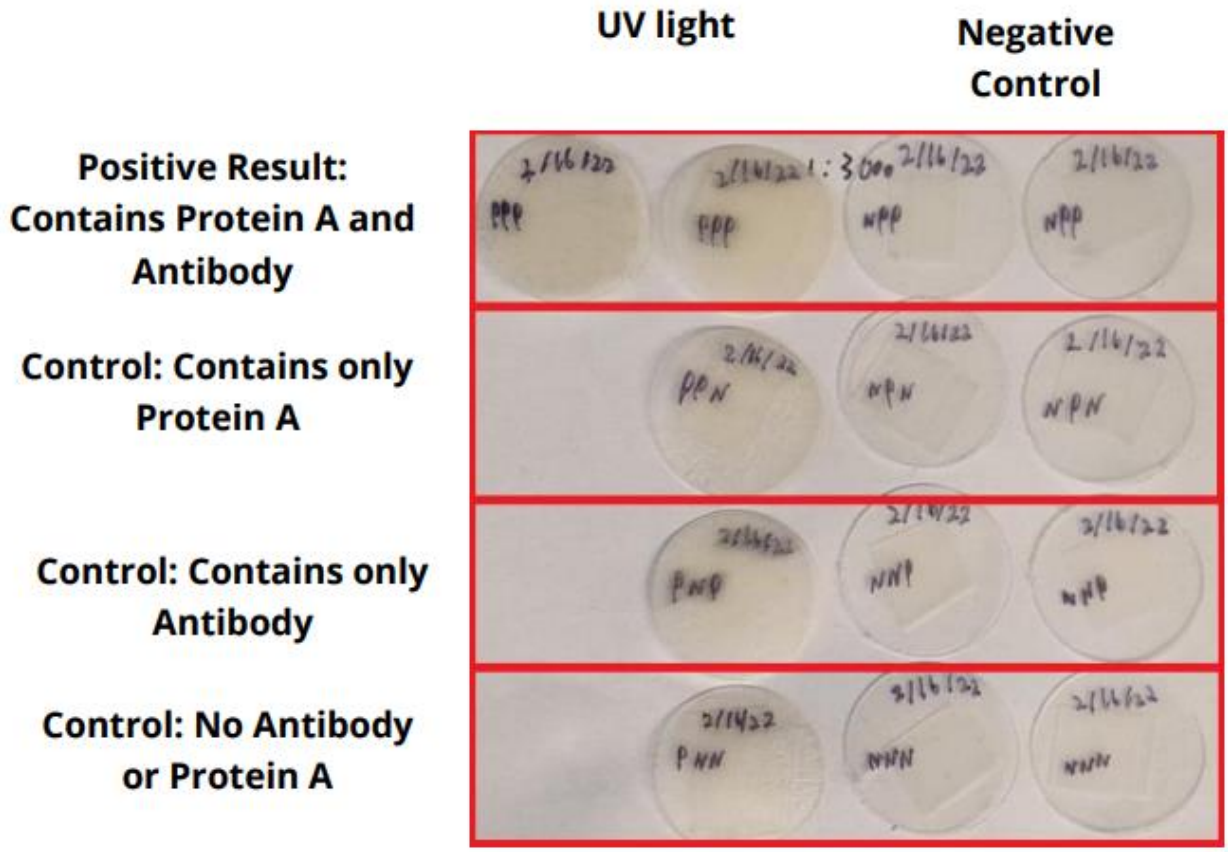

Fig. 14. These discs were either UV light-treated or untreated (Negative Control), the UV light discs in the first row show some purple color as expected along with the yellow hue that is present in every plate and disc after UV light treatment.

Improved Disc Experiment for Plasma and UV light Discs

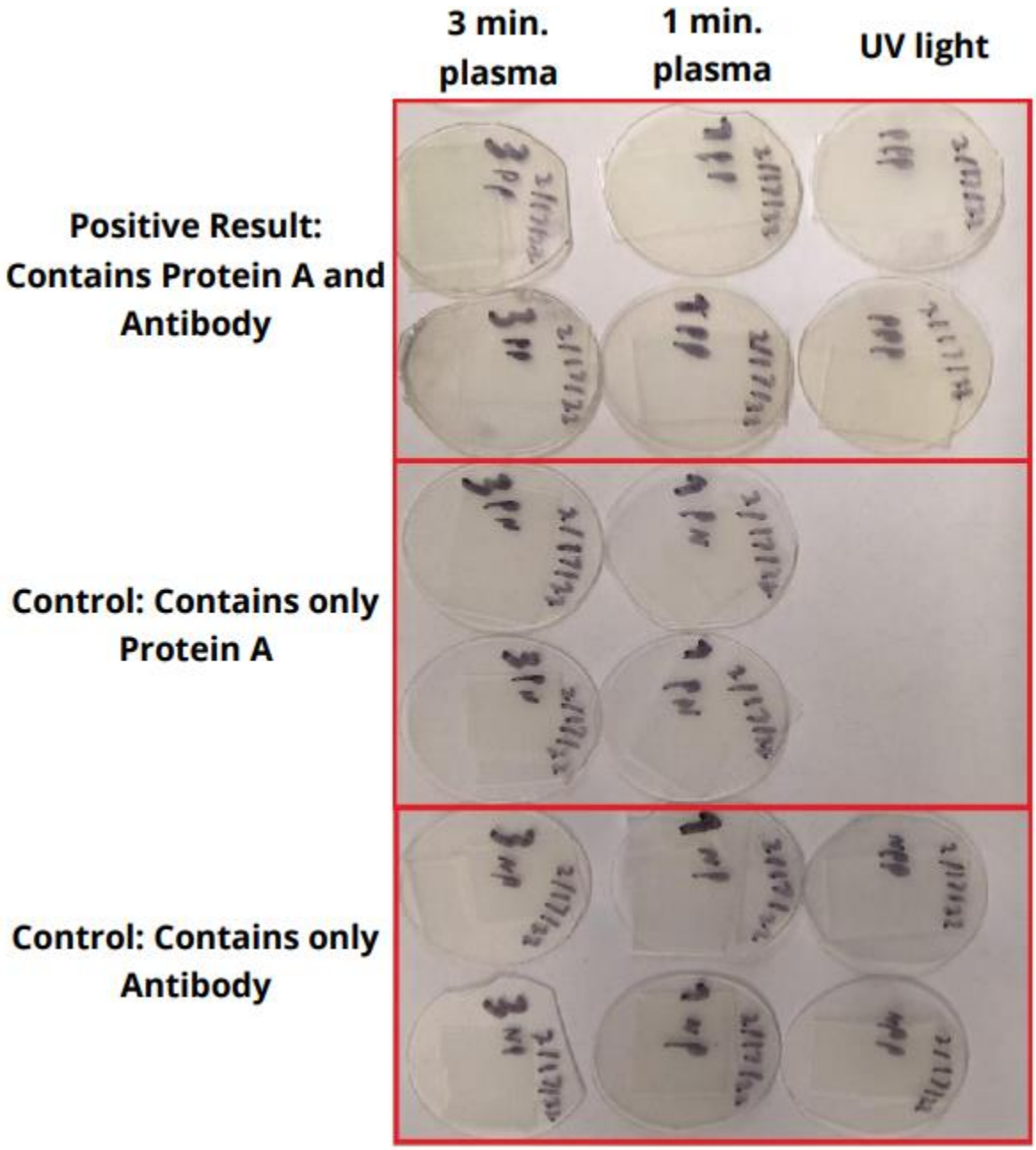

Fig. 15. The first row of this figure shows the dye intensity of plasma and UV light-treated polypropylene discs.

The improvement in dye clarity in **Fig. 14** and **Fig. 15** is likely due to the change in washing from a 1-minute wash with PBS to two 5-minute washes with PBS on a shake station. The control UV light and plasma discs showed little to no purple dye as is expected. No dye was observed in the untreated discs as well. The top row of the discs in **Fig. 15** shows that the plasma discs and UV light discs had similar amounts of dye. The 3-minute plasma-treated disc can be seen to be slightly more dyed than the other discs, although this is not quantitative and only

shows that the treated discs can be used in chromatin immunoprecipitation. As expected, no dye was observed in the control rows.

Water Contact Angle:

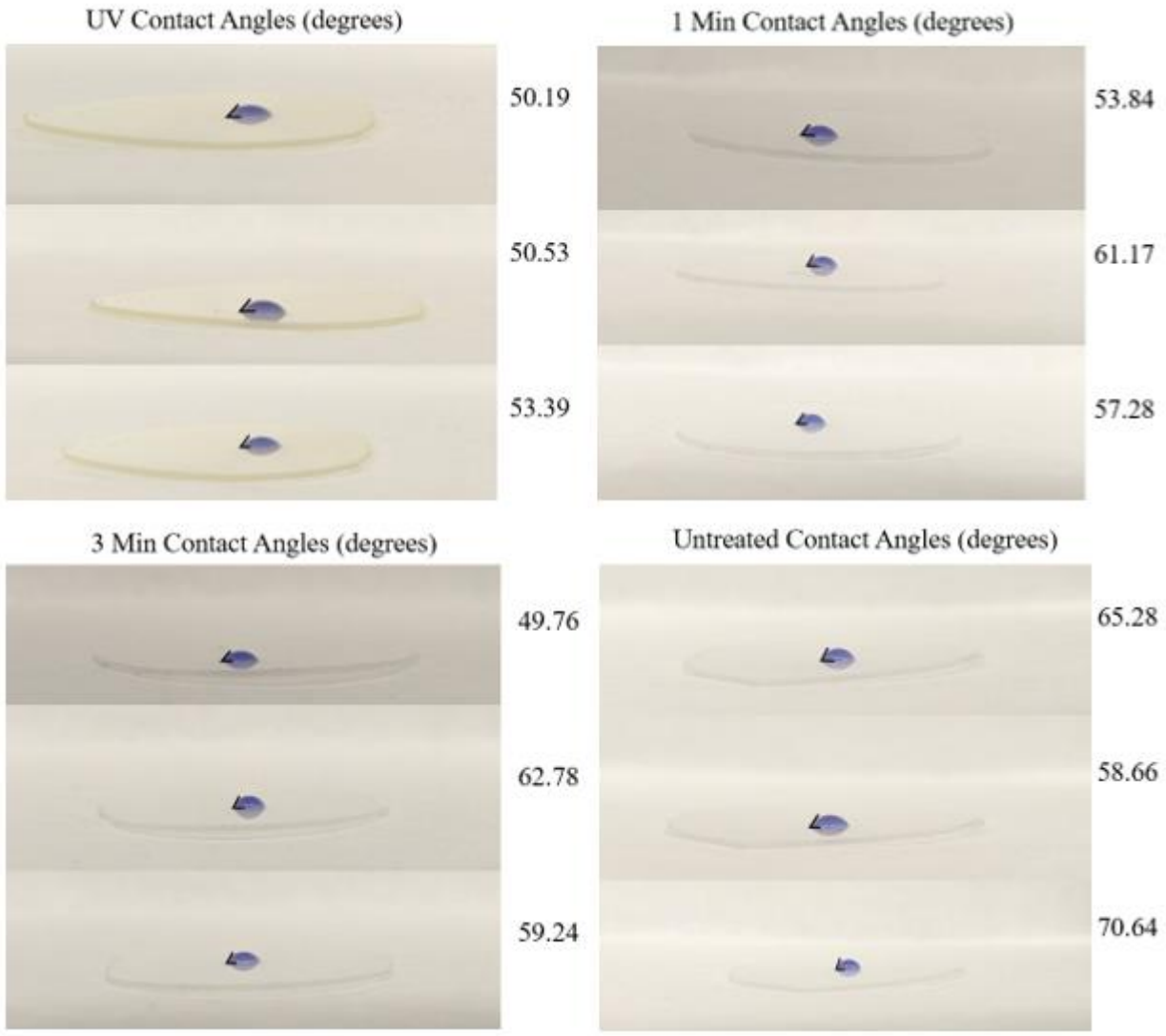

Fig. 16. Three repeated water contact angle measurements on the glossy side of the PP discs treated with UV, 1 min plasma, 3 min plasma, and untreated. 5 uL of Bromophenol blue solution was dropped from the pipette within 1cm of the disc surface. Image data analysis was done with ImageJ.

Fig. 16 shows images taken for WCA measurements on PP discs treated with UV light, 1-min and 3-min plasma along with untreated discs. Direct measurement of each disk reveals the variability that occurs between measurements. The higher angle of the untreated discs can be seen in contrast to the lower angles of the UV-treated discs which resulted in the most consistent measurements of the different treatments.

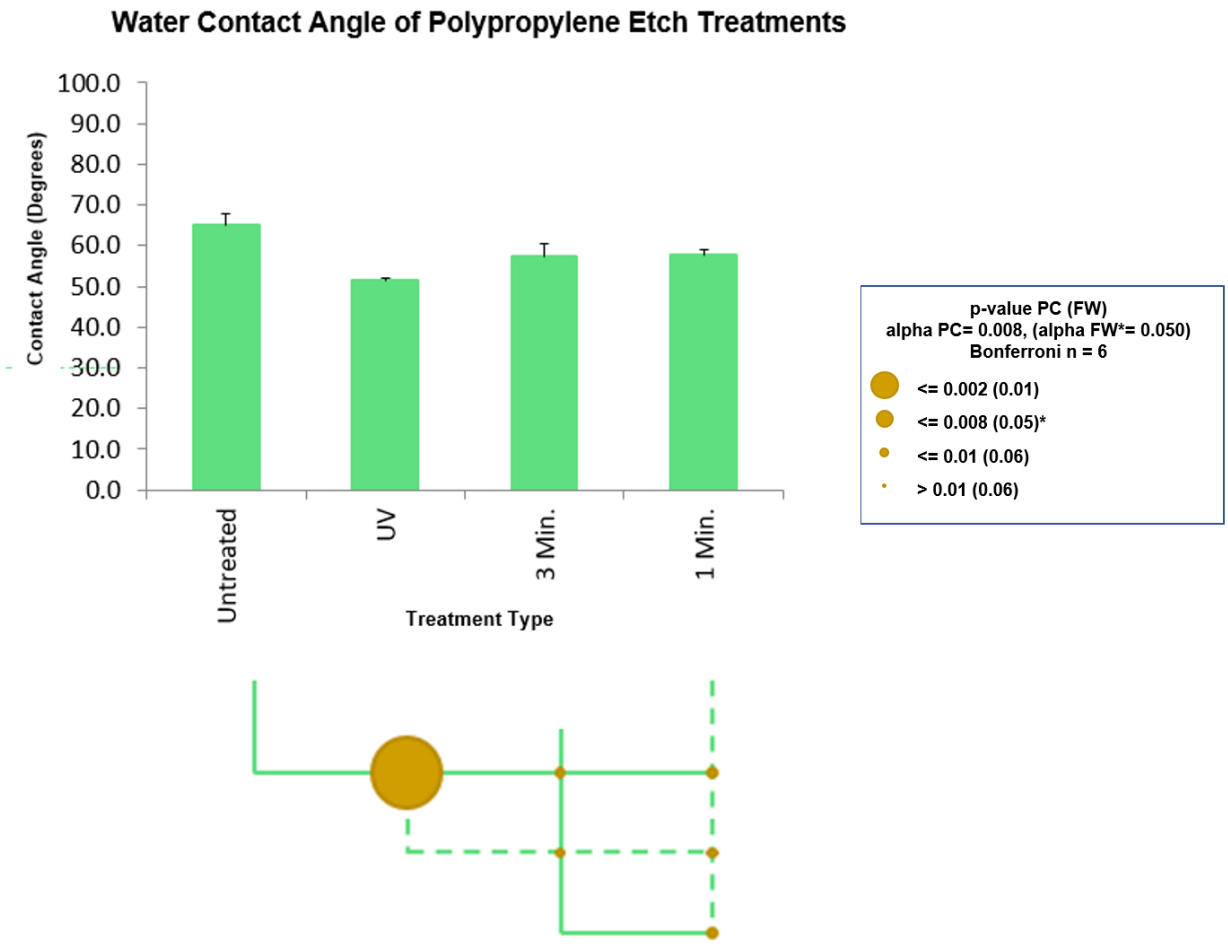

	Untreated	UV	3 Min	1 Min
Average WCA (Degrees)	64.9	51.4	57.3	57.4
Standard Error	2.8	.8	3.2	1.7

Fig. 17. WCA measurements are shown with PP treatment type on the x-axis and WCA measured in degrees on the y-axis. The plot is accompanied by statistical analysis and described with a key on the right. Below are the tabulated results of the data presented in the plot.

The compiled results from the water contact angle experiments are shown in boxplot and numeric form with a Bonferroni statistical analysis as well **(Fig. 17)**. As seen in the statistical

analysis, the UV treatment decreases the WCA of PP plastic surfaces by 13.5 degrees compared to untreated PP. This difference in WCA can be represented as a 20.8 percent (13.5/64.9 degrees) decrease in water contact angle which can be equated to the treatment making the PP surface 20.8 percent more hydrophilic. The decrease in WCA is less for the two plasma treatments. The 1 min treatment causes a 7.5-degree decrease in WCA, and the 3 min treatment causes a 7.6-degree decrease equating to approximately an 8.5 percent decrease in WCA and an increase in hydrophilicity. By WCA metrics the UV treatment leads to a 12.3 percent higher increase in hydrophilicity on PP surfaces than either plasma treatment did. The error in WCA measurements was very low for UV treatment while slightly higher for the plasma treatments and untreated measurements but remained under 3.5 degrees of error, approximately half of the change in WCA for the plasma treatments. While all treatments resulted in changes that are interpreted as increased hydrophilicity, the UV treatment results in statistically significantly higher hydrophilicity. Plasma treatments on the other hand did not have statistically significant increases in hydrophilicity but did show some moderate increase.

XPS Chemical Survey:

XPS survey and Hi-Res XPS survey Combined Plots:

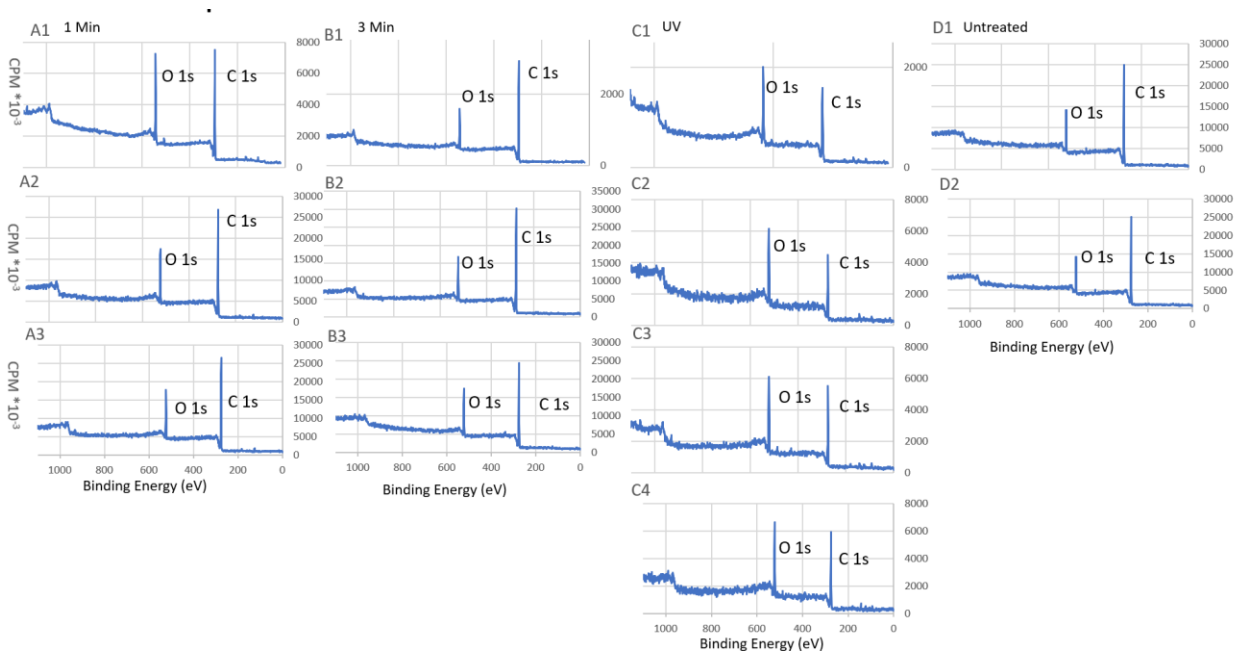

Fig. 18. Y-axis, CPM (counts per minute) measures the number of electrons detected over time from the 800-um square sample area. X-axis, the BE of the detected electrons measured in eV shows which species is present by the graphical curves that form. Plots are ordered 1 Min (A), 3 Min (B), UV (C), Untreated (D), and numbers denote replicates.

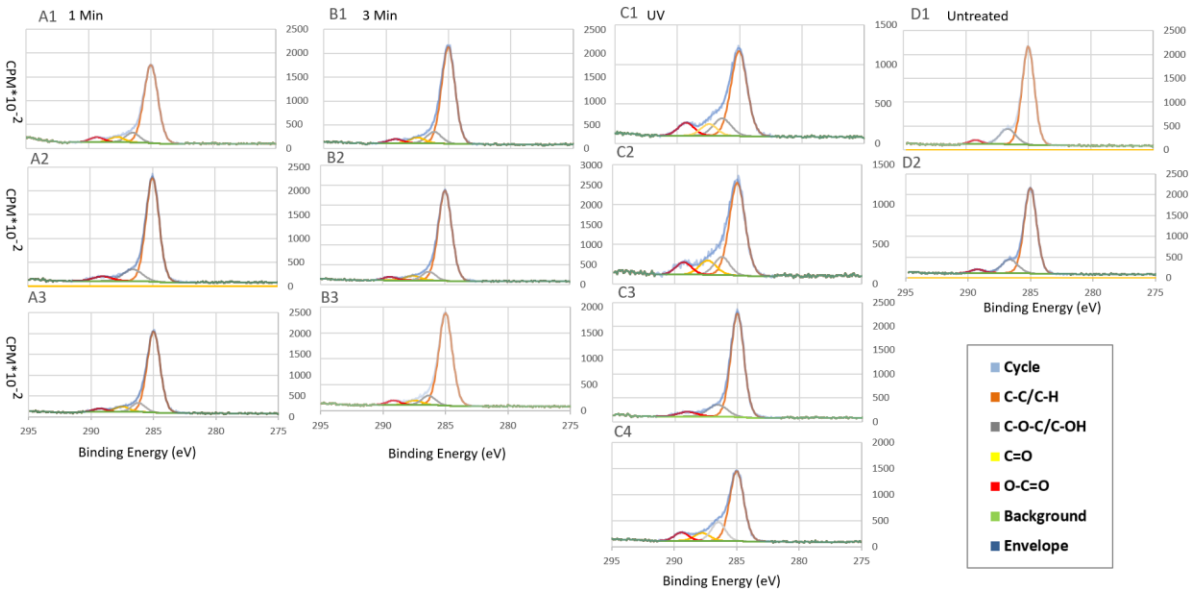

Fig. 19. Similarly, as in **Fig. 18**, the y-axis is in CPM and the x-axis is in BE. The first line is the cycle which corresponds to the direct count of electrons like the XPS surveys in **(Fig. 18)**. The next four lines in the legend are the carbon and oxygen species that curve fitting is done to determine the amount of each species in the cycle. The background represents the value corresponding to the background noise on either side of the cycle curve that is removed. Finally, the envelope is the average line of the cycle which provides the values that are used to fit the curves. Some high-resolution plots were unable to accurately fit the second species, C-OH, in the curve fitting. To remedy this the third species was omitted, C=O, meaning that there was a comparatively small amount of the third species present that is omitted in the 1 min and Untreated statistical analysis below. The plots where this occurred show an orange line at 0 to represent the omitted species (A2, C3, D1, D2).

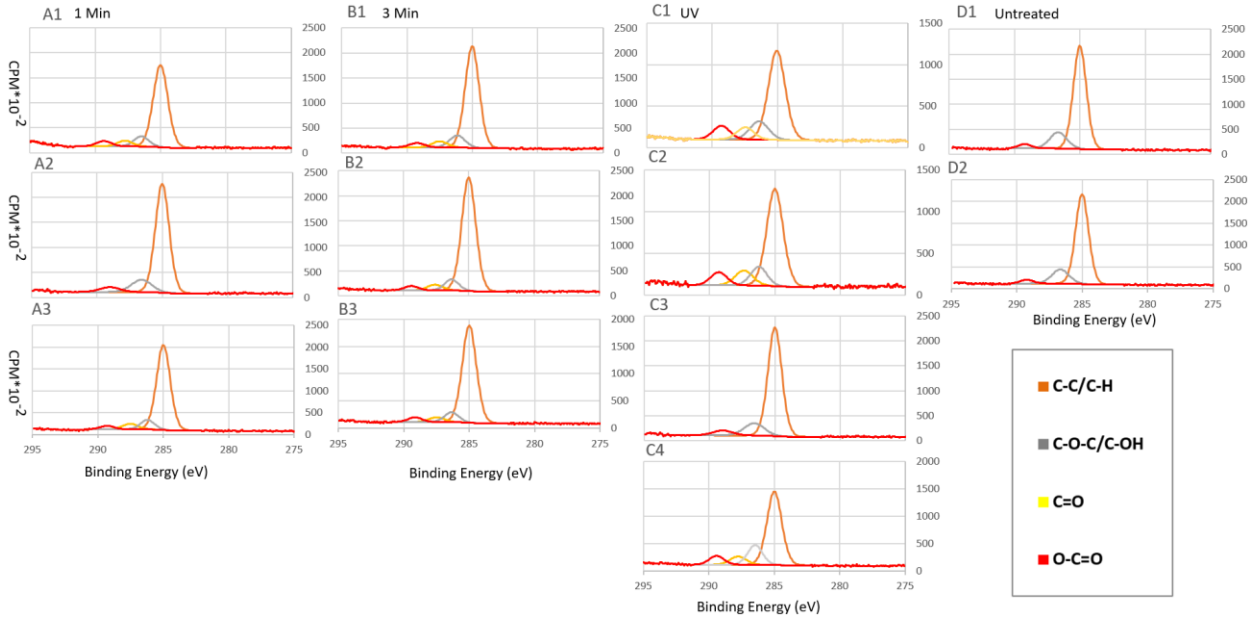

Fig. 20. This figure is the same as the previous plot except with only the chemical species lines represented for better visualization of the differences in the three oxygen species curves.

The survey and Hi-res plots provide some indication of the results of the different treatment type's impact on surface chemistry but are less quantitative than averaged area data **(Table 2 and Fig. 21)** as the area under the curve is the measurement for percent surface area of that chemical. The original survey plots in **Fig. 18** show the total spectrum measured of a wide range of binding energies. This encompasses the labeled oxygen peaks as well as background measured and minor peaks of chemicals in some plots as shown in the tabulated plots as well. The untreated plots show that carbon is much higher than the measured oxygen even without the background removed from the oxygen peak. The 1 min plasma treated PP did have one high value that could be considered a bit of an outlier, but the other two plots do show oxygen approaching or above half the carbon peak. The 3 min-treated PP on the other hand had plots with lower oxygen peaks at or below half the carbon peak. The UV-treated PP on the other hand had a significantly increased oxygen peak which reached above the carbon peak. While this does represent a major success of UV to increase general oxygen content over the other treatments, with the background removed the actual oxygen content is still much below carbon content. The decrease in oxygen content from 1 min to 3 min does show a negative trend in plasma treatment time.

The hi-res C1s plots show carbon spectra of treated PP surfaces that compare the different levels of carbon-oxygen species present in the sample. The C1s region measured by the XPS instrument is focused on a small range of binding energies. This makes the tail of the peak more visible and allows for the average of that peak to be used to estimate the peaks of specific chemical species within the overall peak. The cycle **(Fig 19)** is the direct XPS output, and the background is adjusted to the background noise of eV ranges outside the peaks. The envelope is the average approximation of the cycle with the background removed. The envelope is the polynomial curve that the peaks are calculated from with a Gaussian Lorentzian sum and product functions (GL(30)) which determine the BE (curve position on the plot) and full width at half maximum measurement (FWHM, width of the curve). The peak fitting involved fixing the number of peaks to four species which are the hydrocarbons (C-C/C-H, BE = 285 eV), single-bond oxygen carbon species (C-O-C/C-OH, BE ≈ 286.5 eV), double-bond oxygen carbon species (C=O, BE ≈ 287.5 eV), and double-oxygen carbon species (O-C=O, BE ≈ 289.5 eV). The BE of the peak fitting was fixed at 285 eV for the hydrocarbon peak to use as a reference for the GL(30) calculation, while the BE was allowed to vary for the other three species with oxygen. The FWHM was allowed to vary for all four species ranging from 1.2-1.35 eV. Allowing the position and width to vary make the area under the curve proportional to the percentage of the area on the sample that contained that chemical species. **Fig. 20** more clearly shows the results of the peak fitting and follows a somewhat similar trend to what was seen for the different treatment types in the XPS survey plots. Most of the UV-treated PP plots show all three of the oxygen species as high relative to the hydrocarbon curve. **Fig. 20 C1** and **C2** also show very high levels of the higher bond and oxygen quantity species. The untreated discs showed decently high levels of the single-bond oxygen species but not much of the double-bond and double-oxygen species. The 1 min treated plasma has slightly lower oxygen species peaks

than the UV does and the 3 min treated plasma has even lower peaks. It is more challenging to see qualitative results in these plots than in the XPS survey plots except for the clear carboxyl peaks seen for the UV-treated samples.

XPS Chemical Species	1 min (% area)	3 min (% area)	UV (% area)	Untreated (% area)
O 1s	19.5	15.8	28.0	13.5
C 1s	77.6	83.5	67.5	86.1
Ca 2p	0	0.2	0	0.3
Si 2p	0.9	0	3.4	0
P 2p	1.7	0.5	0.85	0
Na 1s	0.2	0	0	0

Hi-Res Chemical Species	1 min (% area)	3 min (% area)	UV (% area)	Untreated (% area)
C-C/C-H, BE = 285 eV	81	84	68	80
C-O-C/C-OH, BE ≈ 286.5 eV	10	5	11	16
C=O, BE ≈ 287.5 eV	5	8	13	0
O-C=O, BE ≈ 289.5 eV	4	3	8	3

Table 2. Shows tabulated results of compiled average chemical species content for the XPS survey and hi-res C1s as percentage values.

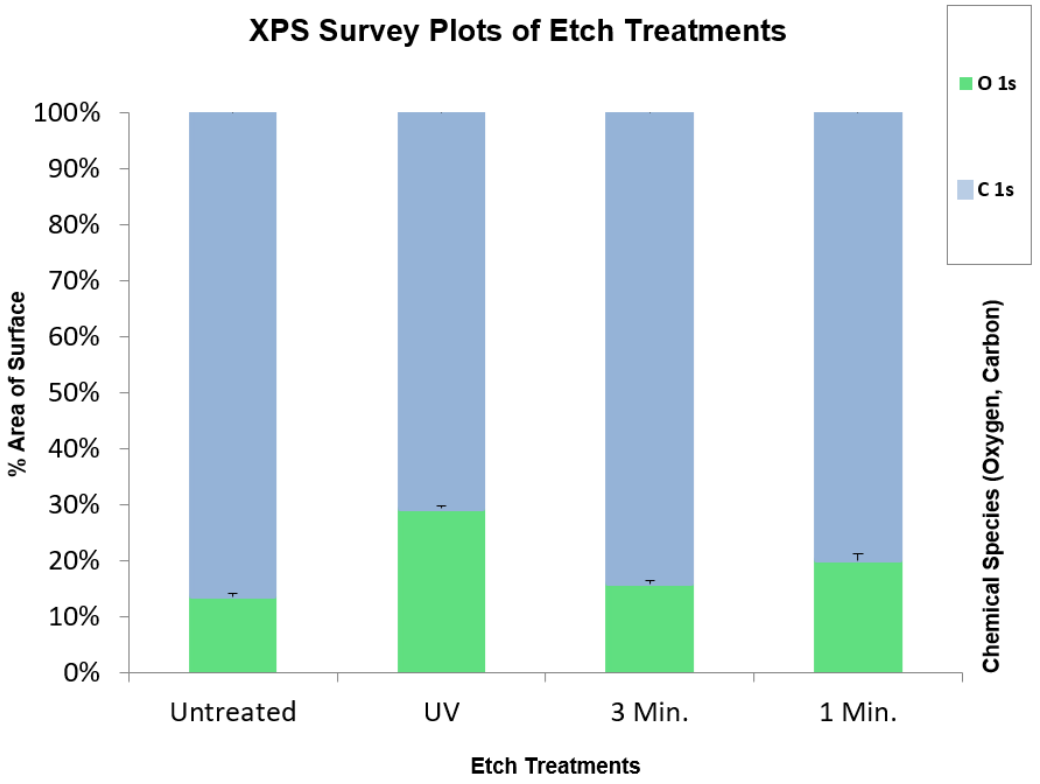

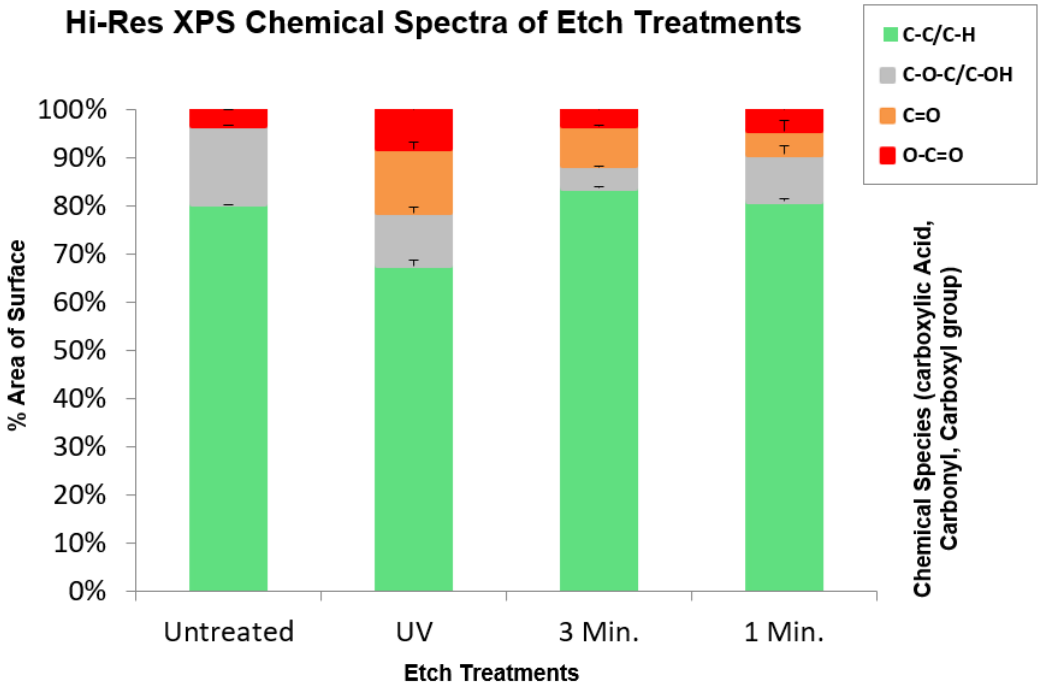

Fig. 21. These plots show the compiled data from the XPS measurements for the various PP treatment types. Both plots have the percent area of the surface on the y-axis as the percentage of the sample area taken up by that chemical species on the surface. The XPS plot has general oxygen and carbon measured including a wide range of

species with those atoms present. The hi-res survey shows the proportion of oxygen species and hydrocarbon bonds measured with various colors.

The combined results **(Fig. 21)** and tabulated **(Table 2)** results give a clearer and more quantified view of the data and trends seen in the survey plots. The untreated PP discs did have some oxygen present at about 13.5 percent of the surface. The UV-treated discs showed a major increase in oxygen content on the surface as seen with the basic XPS survey data, where the oxygen increased by 14.5 percent almost doubling the oxygen. The experimental plasma plates on the other hand saw a smaller increase in oxygen content after treatment. The 3 min plasma plate only saw a 2.3 percent increase in oxygen content, the 1 min plater however had a more moderate increase in oxygen content of 6 percent. The change in carbon content from the treatments largely reflects the change in oxygen content inversely.

The hi-res XPS data **(Fig. 21)** imply that the values for hydrocarbon bonds are almost the same for 3 min and UV plates as the carbon measured in the XPS survey but is higher for the 1 min and lower for the untreated plates. This could be due to errors in the measurements and the hi-res only looking at those species as opposed to some of the other chemicals seen on the surface in the XPS survey. The C-OH content is the basic oxygen species examined and showed a decrease in the content of this species in every treatment type, especially in the 3 min plasma plate with an 11 percent decrease in this oxygen species. The UV and 1 min treatments only saw a 5 and 6 percent decrease in this species. The C=O species had 0 measured percent in the untreated discs which is due to the curves being unable to fit the C=O species accurately with the C-OH curve so there is some C=O present in the sample but very low and is added to the total of the C-OH species. This is also the case for one of the four UV discs and one of the three 1 min discs. The UV plate had a much higher percent increase in C=O species at 13 percent. The 3 min disc had more of this species having 8 percent while the 1 min disc only had 5 percent. The actual percentages for the 1 min and UV treatments would be slightly higher due to the excluded curves. The last species, O=C-O, has the most oxygen and the most polarity. There is a small 3 percent of the surface of untreated discs. The 3 min plasma treated has the same measurement, the 1 min treated has 4 percent and the UV treated has an increase to 8. These small increases show that changes in this species are on a smaller scale than with the other species, but UV still comes out on top almost doubling this percentage after treatment. There is still a minor trend with much error of a small increase in content for the 1 min plasma treated discs. The XPS survey boxplot shows visually the increase in oxygen slightly for the 3 min more for the 1 min and majorly for the UV. In the hi-res plots, the UV plate shows major increases in higher bond and oxygen quantity species and total oxygen content. While the 1 min is missing a lot of the double bond oxygen species content it does show an overall higher amount of general oxygen and double-oxygen species than in the 3 min treatment.

The minor chemical species can impact wettability and include calcium, silicon, phosphorous, and sodium. The calcium and sodium are very low in every sample and can represent common surface contaminants at this level. The silicon and phosphorous content are

more significant and are high for the UV and 1 min plasma-treated discs. The 1 min plasma discs had twice the phosphorous content that the UV discs did, while the UV discs had much higher silicon content. These two species likely represent oxygenated phosphorous and silicon on the surface of the material. These chemicals are not present in the untreated discs and are added by the treatment. The 3 min plasma treatment has no silicon and has lower phosphorus than the UV discs. Both silicon and phosphorous can impact surface wettability depending on bond-dependent interactions between a large amount of oxygen and hydrocarbons on the plastic surface [15, 16]. After treatment of all disc types phosphorous and silicon content are significantly increased especially for UV and 1 min plasma which does not occur in untreated discs. Storage and transportation methods are the same between each treatment and control. This means the only likely sources of contamination are the UV treatment box and the Plasma Reactor chamber at the WNF. These small percentage species could impact the surface wettability beyond the large impact of oxygen species and while they have similar binding energies phosphorous has a higher BE than silicon meaning that phosphorous could be more impactful at improving wettability [17].

In sum, the XPS showed that UV treatment resulted in the highest amount of oxygen on the PP surface and the highest amount of the double-bond and double-oxygen species as well. While not as much as the UV treatment, the 1-min plasma treatment increased the total oxygen more than the 3-min treatment did. The 1-min also had higher levels of the double-oxygen species but lower for the double-bond oxygen species. These levels match the trend of UV outperforming plasma treatment, and the 1-min treatment slightly outperforms the 3-min treatment for oxygen content.

Profilometer Surface Roughness:

Treated Disc Surface Traces:

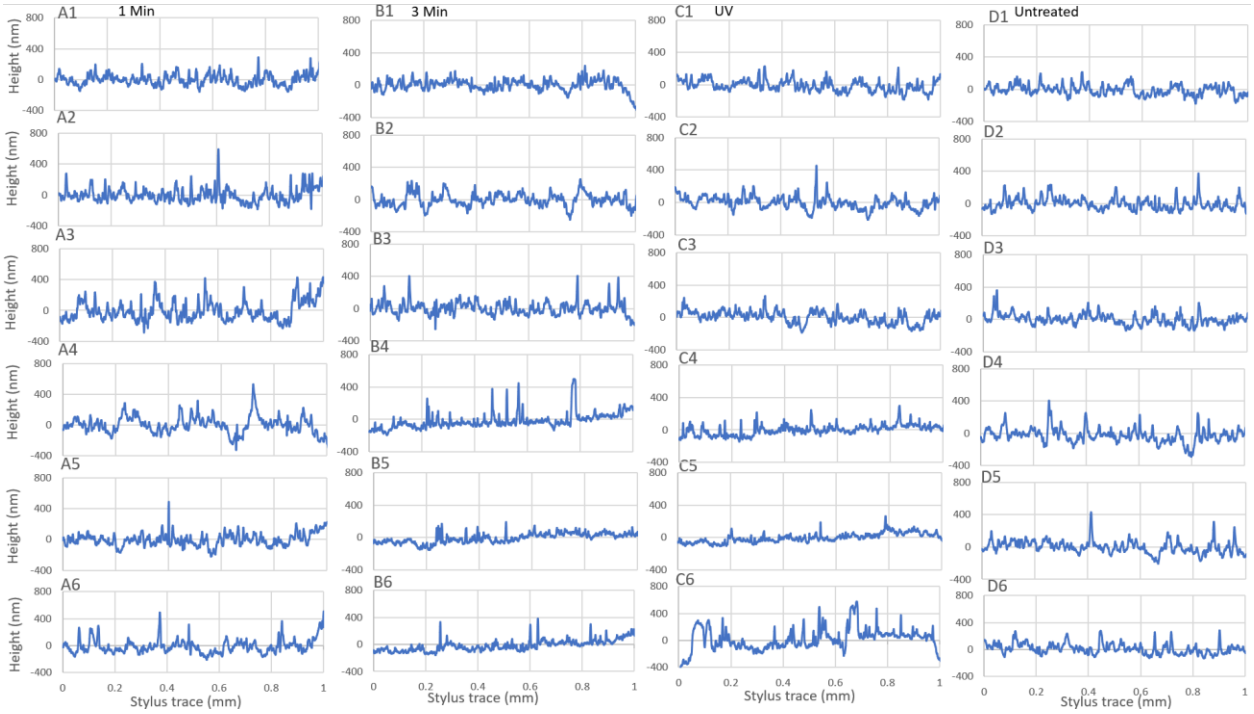

Fig. 22. shows every leveled surface trace plot for the glossy side measurements of the treated discs with the x-axis in mm and the y-axis in nm. The letter at the top left of each plot denotes the treatment type and the number represents the replicate and position used for measurement. 1-3 are the first replicate and 4-6 are the second replicate. 1 denotes the center position, 2 the left position, and 3 the above position which is repeated for 4-6.

The surface traces shown above **(Fig. 22**) do reveal some qualitative features of roughness with obvious peaks and valleys. The 3 min plasma treated and untreated discs can be seen to be very flat in some of their plots but with some variation. The 1 min plasma treated discs do have some especially rough plots and appear to be the roughest. Some of the UV plots are quite flat but overall have some increased roughness in some plots. The trends seen in the surface traces can be seen in the compiled table and plots **(Fig. 23)**. The tabulated results and boxplot show that 1 min plasma treated discs were on average rougher with this analysis method of the locations sampled. The trends seen in the boxplot of average leveled roughness are not statistically significant and only lightly point towards trends in a small sample size. The violin plots **(Fig. 23)** reflect a similar trend with 1 min being the only major increase in roughness from untreated PP. The UV and untreated discs both had a few upper outliers as part of their variability. The error in the 3 min and 1 min is part of a more consistent range.

Levelled Roughness Average	Average roughness	SEM
1 min	76.8	9.4
3 min	31.9	24.1
UV	65.9	14.4
Untreated	60.6	4.8

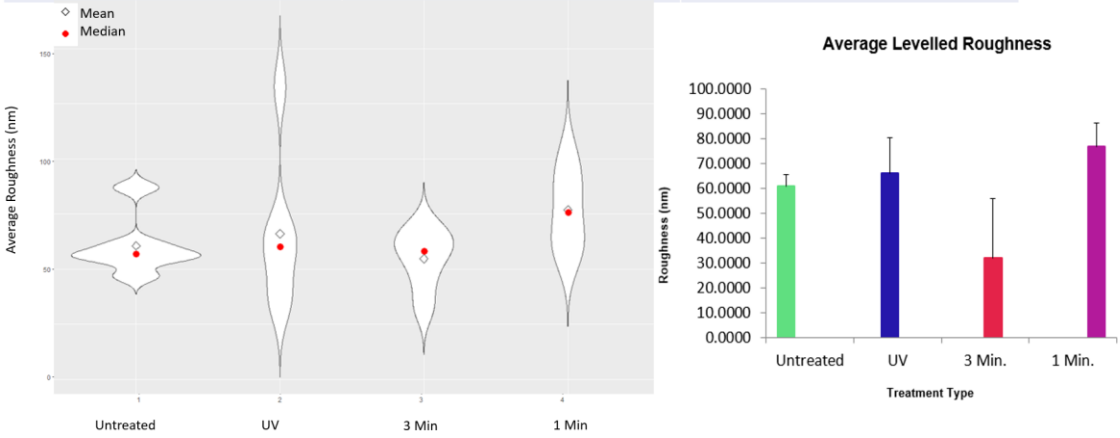

Fig. 23. shows the compiled averages and errors of the average roughness of the treatments. The figure includes the tabulated results as well as a violin plot and boxplot with average roughness on the y-axis measured in nm and the treatment type on the x-axis.

The trend seen in lowered roughness after longer treatment with oxygen plasma etching could indicate that degradation of the surface is occurring but in a way that smooths the surface at an area around the 3 min mark **(Fig. 23)**. The difference between the 1 min treatment and the untreated roughness indicates that roughness does increase from treatment. This limited scope suggests that initial plasma treatment with oxygen does increase the roughness of the PP surface, but longer treatments appear to smooth the surface features and cause less average roughness but with \ wide variations. These trends do match what is seen in the surface roughness of polyethylene (a similar plastic) treated with oxygen plasma etch for 1 3 and 5 minutes where 1 min has increased roughness, which is lowered at 3 min and then begins to increase in roughness with 5 min [9]. Confirmation of part of this trend in PP is useful and suggests that times around 1 min could be explored further for ideal increases in roughness which could then be cross-compared with the ideal plasma treatment time for surface oxygen content and generation of higher bond and oxygen quantity species. Times around 5 minutes could likely be investigated as well since PP is more heat resistant than polyethylene and can withstand that treatment time. The roughness curve might even be slightly shifted for PP due to the differences in material chemistry within the scope of polymer plastics.

Quantitative ChIP Experiments:

ChIP Data for Plate Treatments:

A

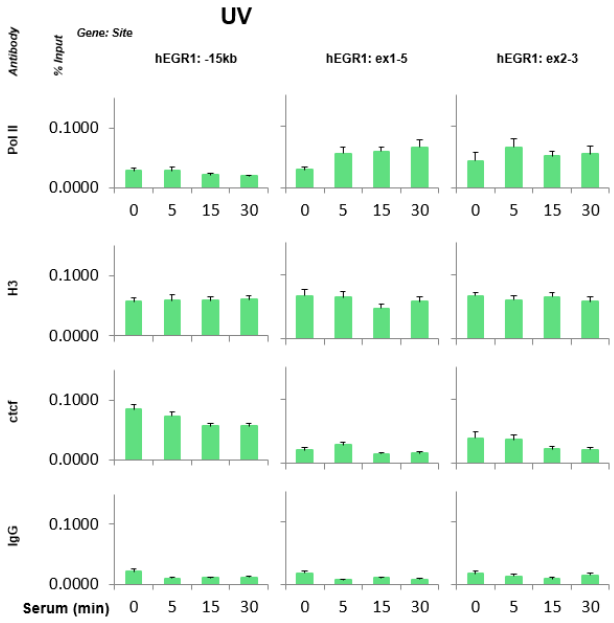

B

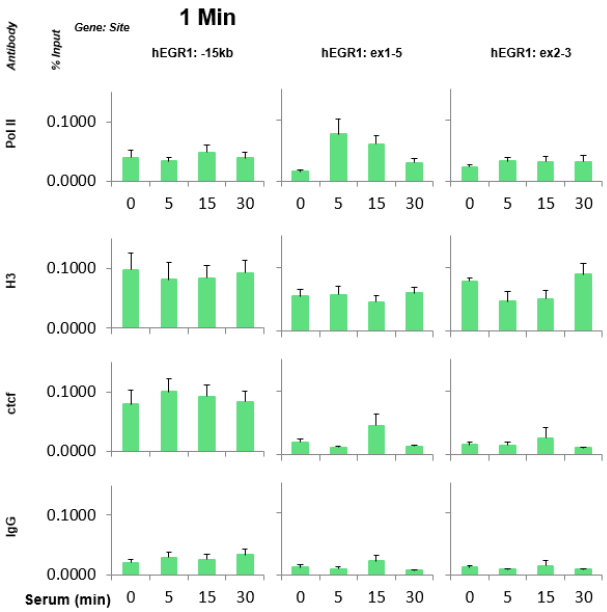

C

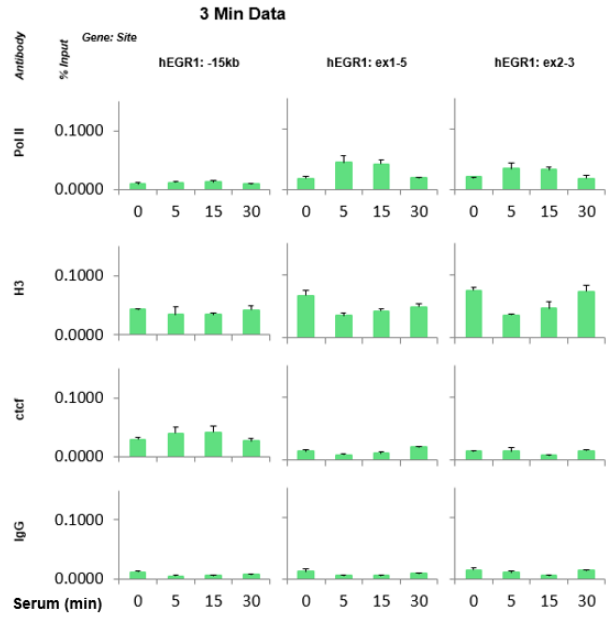

D

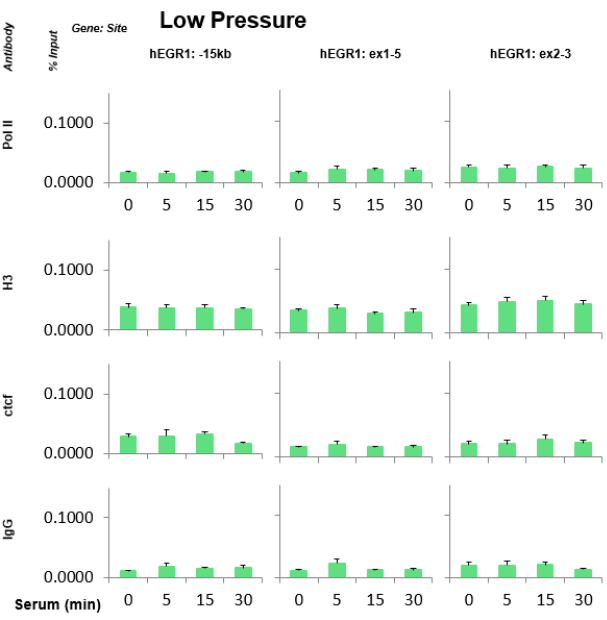

E

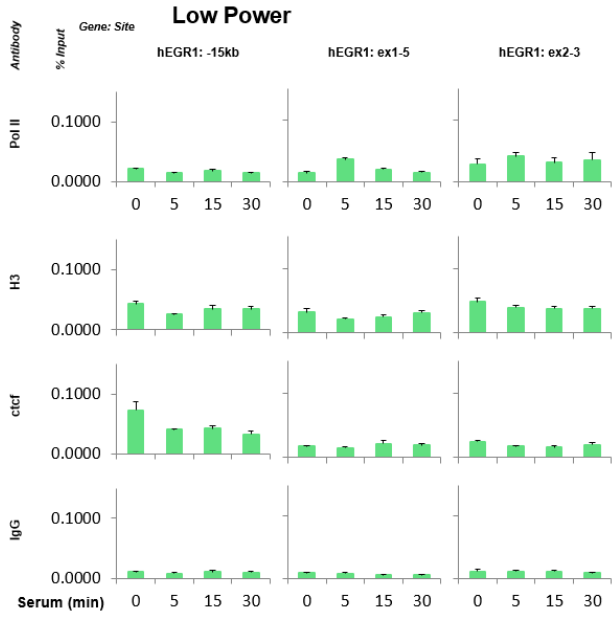
Low Power
Gene: Site
Antibody
% Input
hEGR1: -15kb
hEGR1: ex1-5
hEGR1: ex2-3
Pol II
H3
ctcf
IgG
0.1000
0.0000
0 5 15 30
Serum (min)

F

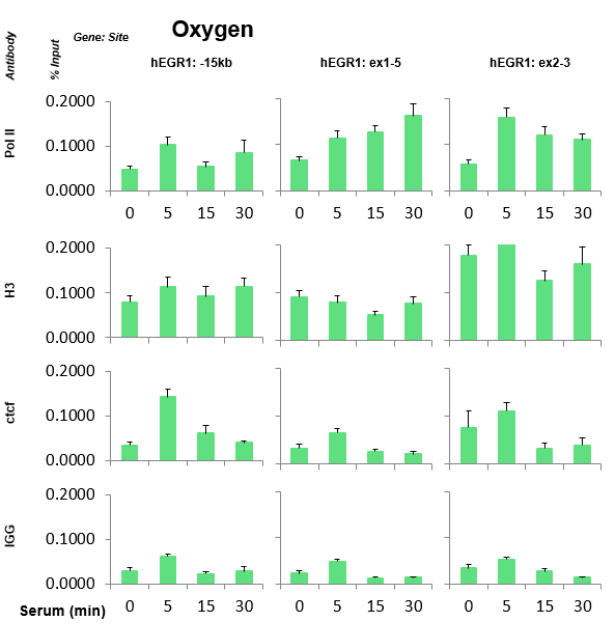
Oxygen
Gene: Site
Antibody
% Input
hEGR1: -15kb
hEGR1: ex1-5
hEGR1: ex2-3
Pol II
H3
ctcf
IGG
0.2000
0.1000
0.0000
0 5 15 30
Serum (min)

G

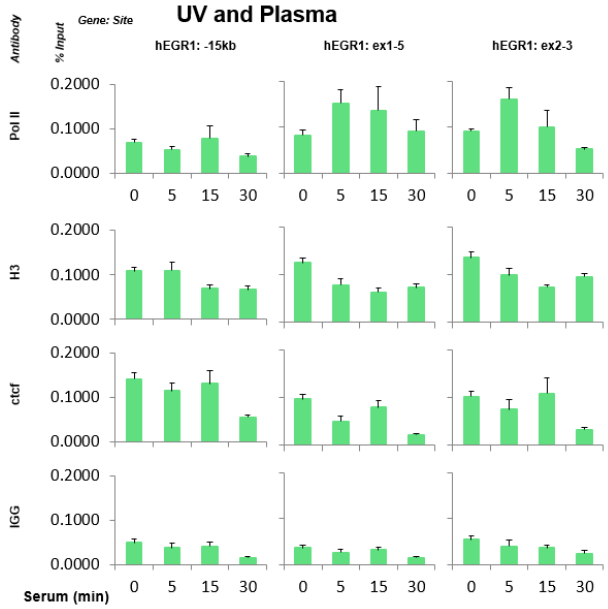
UV and Plasma
Gene: Site
Antibody
% Input
hEGR1: -15kb
hEGR1: ex1-5
hEGR1: ex2-3
Pol II
H3
ctcf
IGG
0.2000
0.1000
0.0000
0 5 15 30
Serum (min)

H

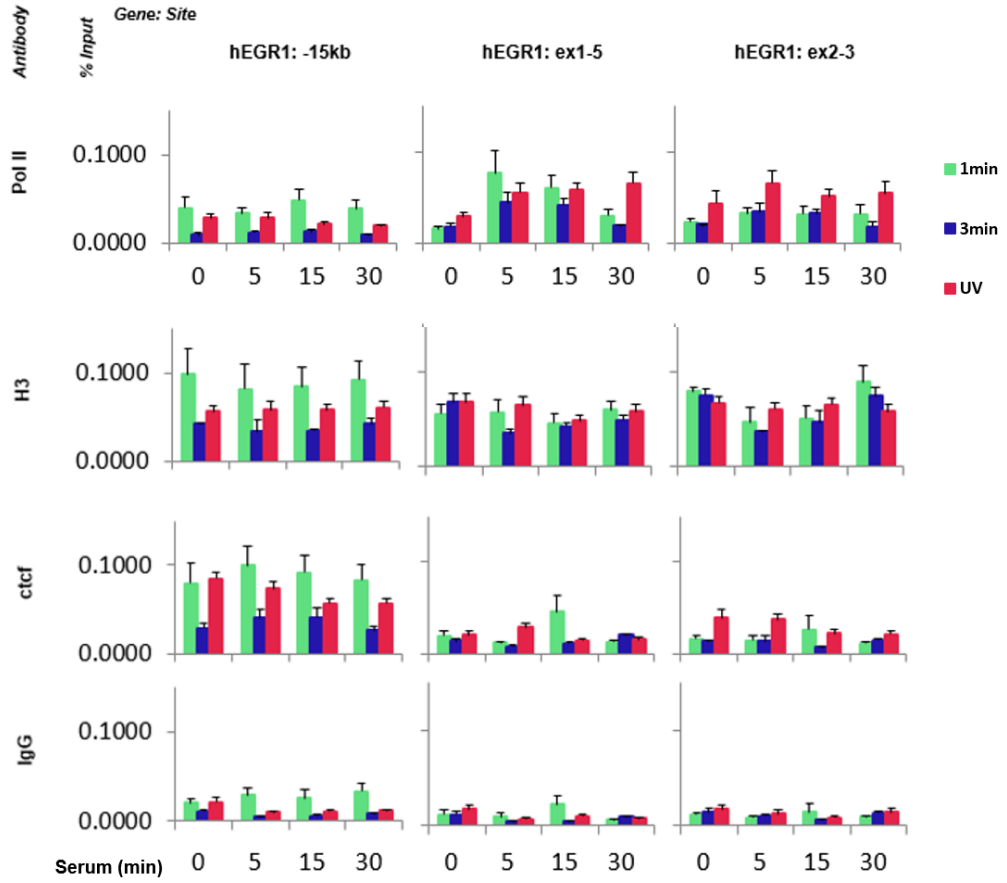

Fig. 24. Shows all combined Matrix ChIP data for each PP treatment type labeled at the top of each dataset beginning with UV control. Included are a compiled comparison of UV 1 min and 3 min plasma treatment datasets side by side at the end. The ChIP data is displayed with the inner and outer axis. The outer y-axis for the dataset denotes the antibody for each plot, the outer x-axis denotes the gene site for each plot. The inner y-axis shows the fraction of input chromatin that is put into the wells that is immunocaptured and then measured. The inner x-axis shows the different serum times that the chromatin was treated with. The replicated assays for each treatment are N = 36 for UV, N = 9 for 1 min, N = 3 for 3 min, N = 6 for low pressure and low power, and N = 9 for high oxygen and UV plasma combined.

ChIP Metrics:	UV (Fraction input)	1 Min (Fraction input)	3 Min (Fraction input)
Pol II peak	0.0654 (± 0.0113)	0.0762 (± 0.0254)	0.0440 (± 0.0116)
H3 average	0.0560 (± 0.0069)	0.0696 (± 0.0161)	0.0481 (± 0.0106)

CTCF peak	0.0844 (± 0.0083)	0.0995 (± 0.0220)	0.0411 (± 0.0065)
IgG average	0.0122 (± 0.0030)	0.0167 (± 0.0055)	0.0086 (± 0.0016)

Background Adjusted ChIP Metrics:	**UV (Fraction input)**	**1 Min (Fraction input)**	**3 Min (Fraction input)**
Pol II peak	0.0532	0.0595	0.0354
H3 average	0.0438	0.0529	0.0395
CTCF peak	0.0722	0.0828	0.0325

Table 3. shows the tabulated results of some key metrics from the ChIP datasets for the main identified treatments. The pol II and CTCF peaks are the highest value in the plots for those antibodies. The H3 average and IgG average are the average value of percent input for each timepoint for those plots. The second part of the table shows the values with the background subtracted.

The ChIP data plots **(Fig. 24)** show the efficiency of chromatin immunoprecipitation (shown as a fraction of input) of PP plates treated with UV and plasma. The UV-treated plates represent the standard serum-induced chromatin changes at the EGR1 gene. ChIP signal intensity is proportional to the density of the protein of interest at the given gene site. On UV-treated plates, the Pol II antibody yielded low immunocapture at the -15kb site but a higher signal response in the other two gene sites especially at serum time points 5-30 min. The H3 antibody shows a consistently moderately high immunocapture at each gene site and time point of serum treatment. This observation matches the expected behavior of H3 as this histone protein is part of nucleosomes that decorate the entire genome. The CTCF antibody reveals a strong signal at the -15kb site, especially at 0-time point serum treatment, and is lower as expected at other EGR-1 sites. The non-immune IgG antibody signal is low at every gene site as it is a measure of unspecific background levels.

ChIP results from 1 min and 3 min plasma-treated plates follow the ChIP data seen with the UV-treated plates. The 1 min plasma treated plates had comparably high Pol II and CTCF signal peaks along with higher background, but less uniform H3 signals. The 3 min plasma treated plates had lower Pol II and CTCF peak signals along with low background and low H3 signals that varied across the different time points. The low-pressure plates demonstrated low

ChIP signals and very little difference between peaks and background. The low-power plates had some low Pol II peaks and decent CTCF peaks along with a very low background and a low H3 immunocapture. The high oxygen-treated plates had high peaks for Pol II and CTCF but also a very high background for these antibodies and for IgG, the H3 ChIP signal was high but inconsistent between the gene sites. The combined UV and plasma-treated plates had high peaks and background levels like the high oxygen-treated plates, the H3 ChIP signal was high but varied significantly across serum time points. Overall, the low-pressure and low-power treated plates have too low ChIP signals and the oxygen and combined treatment plates have too high background signals to be a viable replacement for the UV-treated plates.

The plasma treatments that produced the best results that were as efficient as the UV treatment and demonstrated better signal-to-background ratios were the 1 min plasma treatment and the 3 min plasma treatment. Other treatments did show some indications of trends that could be fine-tuned to produce better-performing plates. The tabulated results **(Table 3)** of the few key metrics give a more quantitative analysis of the benefits and detriments of tested plate treatment types. The background-adjusted average ChIP metrics compare the UV vs. plasma treatments. While the 3 min plasma treatment had lower ChIP metrics than UV, the 1 min plasma treatment surpassed the UV at every ChIP metric. For example, the Pol II ChIP peak was higher in the 1 min plasma by 11.8 percent than in UV. The average H3 ChIP signal was higher in the 1 min plasma by 20.7 percent, and the CTCF ChIP signal was higher by 14.7 percent. The 1 min plasma plate has low IgG signal matching the low background noise of the UV plates.

In sum, the overall analysis of the ChIP data shows the 1 min plasma treatment most closely matches the efficiency of the UV-treated plates and performs 11-20 percent better for some antibodies than UV-treated plates do, and the background can be mitigated by subtracting average IgG values.

Discussion

This study aims to replace slow and hard-to-control UV treatment of plates used in ChIP assay with fast and reliable plasma treatment. Connecting analysis of the PP surface that was modified by plasma to the ChIP data is important to understand the impact of surface treatment variables on assay performance quality. The WCA measures surface wettability, which can be interpreted as surface energy, where a lower angle means higher energy on the surface. This inverse trend corresponds to high energy being represented as highly polar oxygen species in the XPS analysis **(Figs. 21).** The atomic forces that attract the water molecules to the high polarity and high energy oxygen species on the PP surface comprise interactions that link XPS quantitative results to WCA angle measurements [16]. These added polar species provide the additional hydrophilic binding sites for the protein A molecules to bind without denaturing which allows for ChIP to occur which is the connection between surface analysis and ChIP performance.

Both the WCA and XPS surface analysis methods revealed differences between the UV and plasma treatments. While changes and trends in the plasma are small for the XPS data, they do point towards a general increase in surface oxygen content after just 1 min of plasma treatment. The 3 min plasma treatment did have higher of the second oxygen species than the 1 min did but less of the third oxygen species **(Figs. 19, 20, and 21)**. Altogether the data shows that the UV treatment does outperform the plasma treatments at adding general oxygen and proportionally adding higher bond and oxygen quantity species. The second and third oxygen species are more important to increase the surface energy of the PP as they are more polar molecules and most important for protein A binding to the surface in ChIP assay. This reinforces the trend that plasma can increase oxygen content, but UV is stronger in these treatments as demonstrated trends in the WCA measurements **(Fig. 17)**.

The roughness estimation measurements **(Fig. 23)** show that there is some increase in average roughness in the UV and 1 min treated PP compared to untreated PP with these collection and analysis methods. The 3 min-treated plasma showed a significant decrease in average roughness. The 1 min plasma PP had a slightly higher average roughness than UV. These results could be considered inconclusive due to low statistical significance or that there are only minor changes in roughness from etching treatment on this material. The original premise of the increased surface roughness was enlarging the area for the protein A molecules to bind and increase antibody binding capacity. The original premise could be missing larger factors at play that the new surface area from the treatment may have fewer or perhaps much fewer sites where higher bond and oxygen quantity oxygen species are added to the surface. Without the added oxygen sites the new surface area of the generated roughness from the treatment may have similar qualities to untreated PP and lack an increased capacity for protein binding. There is the possibility that roughness is generated at locations where oxygen is added as plasma etching, and UV light involves adding oxygen through high-energy transfers of radical atoms. These molecular additions could be the cause of profile changes in the material but represent a small fraction of the total molecular additions. Overall, if there is no major change in roughness from etching treatments, then the etching treatment mainly increases hydrophilicity and ChIP signal through increased amounts of highly polar molecular sites.

The ChIP data **(Fig. 24)** showed that the 1 min plasma treatment resulted in the highest signal-to-background ratio while mimicking the efficiency of the UV-treated plates. The 1 min plasma treated plate had low unspecific background noise and showed improvement in background adjusted peak signals by 11. 8 and 14.7 percent over UV treatment and a general signal improvement of 20.7 percent **(Fig. 24A and B)**. These improvements seen in the ChIP data do not directly match up with the lower oxygen and higher WCA seen in the 1 min plasma-treated PP than in the UV-treated PP. This discrepancy could point towards surface characteristics differences between UV and plasma treatments. This difference could be due to the measured roughness being higher in the 1 min plasma treatment than in UV, but this is inconclusive. Alternatively, it could be due to the other chemical species, for example,

phosphorous has higher energy than silicon and there is more phosphorous after the 1 min plasma treatment and more silicon after the UV treatment. These trends point towards a potential link between surface chemical modification and ChIP performance, meaning that surface analysis experiments can be used to rapidly test other variations in plasma treatment protocols to identify key treatments to test in ChIP experiments. While they are not absolute quantifications of ChIP performance, they are predictive within error as seen with the discrepancies between 1 min and UV. These surface analysis methods will save significant amounts of resources and lab work by eliminating the need to do many ChIP experiments with treatments that might not offer any benefit. It will allow the best plasma treatment method to be determined and the 1 min plasma treatment shows promise and the right direction for further improving assay performance. The 1 min plate could replace UV currently if further testing sees reliability for other antibodies since IgG can be subtracted to remove background ChIP binding. The difference between the plasma plates of 1- and 3-min treatments point towards treatments of less than 1 minute could yield higher signal peaks without significantly increasing the background levels **(Fig 24B and C)**. Other identified avenues of investigation for better plate treatment methods are to test a panel of slightly higher oxygen values or lowered power settings to determine the ideal treatment for ChIP performance. Another gas besides oxygen that could prove some benefit is argon which can be used to increase the surface roughness of a material [9] without being as reactive as oxygen is. Combined argon oxygen treatments could be tested to determine if there are significant increases in roughness and if that benefits ChIP efficiency.

One of the most important future projects once an ideal plate treatment method has been identified will be performing Next Generation Sequencing (NGS or seq). The 1 min plasma already shows promise of outperforming the UV treatment method if the response seen with the antibodies and gene sites in this experiment matches the efficiency seen with other antibodies and gene sites. NGS is expensive and challenging so it will need to be performed with care. Matrix-ChIPed DNA will be used to generate libraries for sequencing. Matrix-ChIP-seq experiments are expected to provide more insights into the performance of the plasma-treated plates compared to UV-treated plates for a much wider range of antibodies and sites. The increased ChIP efficiency from the ideal plasma treatment will allow for a greater range of antibodies that can be used to study chromatin samples and benefit cancer research. The improved assay performance of the plate will allow for the high-throughput PIXUL Matrix-ChIP to better study large repositories of cancer samples accelerating and expanding cancer research.

Acknowledgments:

Many thanks and acknowledgments go to the following individuals for assistance with this thesis project.

- Dr. Karol Bomsztyk – PI and primary advisor
- Dr. Lara Gamble – Committee advisor
- Dr. Oleg Denisenko – Committee advisor

- Daniel Mar – Lab technician, lab procedure training
- Dr. Mark Morgan - Dry etching engineer at Washington Nanofabrication Facility
- Dr. Samantha Young – XPS faculty expert at UW Molecular Analysis Facility
- Bomsztyk lab group

References:

[1]
R. L. Siegel, K. D. Miller, H. E. Fuchs, and A. Jemal, “Cancer Statistics, 2021,” CA: A Cancer Journal for Clinicians, vol. 71, no. 1, pp. 7–33, Jan. 2021, doi: 10.3322/caac.21654.
[2]
World Health Organization: WHO, “Cancer,” *Who.int*, Mar. 03, 2021. https://www.who.int/news-room/fact-sheets/detail/cancer
[3]
K. Bomsztyk et al., “PIXUL-ChIP: integrated high-throughput sample preparation and analytical platform for epigenetic studies,” Nucleic Acids Research, vol. 47, no. 12, pp. e69–e69, Mar. 2019, doi: 10.1093/nar/gkz222.
[4]
S. Flanagin, J. D. Nelson, D. G. Castner, O. Denisenko, and K. Bomsztyk, “Microplate-based chromatin immunoprecipitation method, Matrix ChIP: a platform to study signaling of complex genomic events,” *Nucleic Acids Research*, vol. 36, no. 3, p. e17, Feb. 2008, doi: 10.1093/nar/gkn001.
[5]
D. Mar *et al.*, “MultiomicsTracks96: A high throughput PIXUL-Matrix-based toolbox to profile frozen and FFPE tissues multiomes,” Mar. 2023, doi: https://doi.org/10.1101/2023.03.16.533031.
[6]
National Institutes of Health. “PIXUL-FFPE: High throughput platform for chromatin and DNA sample preparation from formalin fixed paraffin embedded (FFPE) tissue samples.” *Nih.gov*, 2021. https://reporter.nih.gov/search/pv3ZrOf48k6EXXA8FXjabw/project-details/10021842#similar-Projects.
[7]
National Institutes of Health. “Next generation technology to detect epigenetic alterations in human tissues” Nih.gov, 2021. https://reporter.nih.gov/search/pv3ZrOf48k6EXXA8FXjabw/project-details/9221293#similar-Projects.
[8]
D. Jensen, K. Bomsztyk, “Increasing Antibody Binding Capacity of Polypropylene 96-well Plates used in Matrix Chromatin Immunoprecipitation”. University of Washington capstone June 2019.
[9]
Spyrides, Silvana Marques Miranda, et al. “Mechanism of Oxygen and Argon Low Pressure Plasma Etching on Polyethylene (UHMWPE).” Surface and Coatings Technology, vol. 378, Nov. 2019, p. 124990. ScienceDirect, https://doi.org/10.1016/j.surfcoat.2019.124990.
[10]
Starlab. “96-Well PCR Plate, Skirted, Low Profile, White - STARLAB,” *Starlabgroup.com*, 2023. https://www.starlabgroup.com/en/product/96-well-pcr-plate-skirted-low-profile-white-e1403-5209.html
[11]
Mandolfino C, Lertora E, Gambaro C, Pizzorni M. Functionalization of Neutral Polypropylene by Using Low-Pressure Plasma Treatment: Effects on Surface Characteristics and Adhesion Properties. *Polymers*. 2019;11(2):202. doi:10.3390/polym11020202

[12]
T. P. Ferguson and J. Qu, “Moisture and temperature effects on the reliability of interfacial adhesion of a polymer/metal interface,” Electronic Components and Technology Conference, Jun. 2004, doi: https://doi.org/10.1109/ectc.2004.1320355.
[13]
H. Chen, J. L. Muros-Cobos, and A. Amirfazli, “Contact angle measurement with a smartphone,” *Review of Scientific Instruments*, vol. 89, no. 3, p. 035117, Mar. 2018, doi: https://doi.org/10.1063/1.5022370.
[14]
Mitutoyo. “QUICK GUIDE TO SURFACE ROUGHNESS MEASUREMENT Reference guide for laboratory and workshop SURFACE ROUGHNESS.” Available: https://www.mitutoyo.com/webfoo/wp-content/uploads/1984_Surf_Roughness_PG.pdf
[15]
Artur Kudyba, N. Sobczak, A. Siewiorek, and R. Kozera, “Effect of phosphorus content on the wettability of Ni-P coated surfaces by SAC305 alloy,” ResearchGate, 2014. https://www.researchgate.net/publication/281237707_Effect_of_phosphorus_content_on_the_wettability_of_Ni-P_coated_surfaces_by_SAC305_alloy
[16]
A. Bellel, S. Sahli, Z. Ziari, Raynaud P, Y. Segui, and D. Escaich, “Wettability of polypropylene films coated with SiOx plasma deposited layers,” Surface & Coatings Technology, vol. 201, no. 1–2, pp. 129–135, Sep. 2006, doi: https://doi.org/10.1016/j.surfcoat.2005.11.100.
[17]
XPS Database. “Phosphorus (P), Z=15, & Phosphorus Compounds,” Xps-database.com, Apr. 19, 2022. https://xps-database.com/phosphorus-p-z15-phosphorus-compounds/